DESIGN OF SCREW EXTRUDER FOR THREE-DIMENSIONAL CERAMIC PRINTING

WU PENG

A project report submitted in partial fulfilment of the requirements for the award of Master of Engineering (Mechanical)

Lee Kong Chian Faculty of Engineering and Science
Universiti Tunku Abdul Rahman

January 2021

DECLARATION

I hereby declare that this project report is based on my original work except for citations and quotations which have been duly acknowledged. I also declare that it has not been previously and concurrently submitted for any other degree or award at UTAR or other institutions.

Signature : WU PENG

Name : WU PENG

ID No. : 20UEM00661

Date : 2/4/2021

APPROVAL FOR SUBMISSION

I certify that this project report entitled **"DESIGN OF SCREW EXTRUDER FOR THREE-DIMENSIONAL CERAMIC PRINTING"** prepared by **WU PENG** has met the required standard for submission in partial fulfilment of the requirements for the award of Master of Engineering (Mechanical) at Universiti Tunku Abdul Rahman.

Approved by,

Signature : 

Supervisor : Dr Tey Jing Yuen

Date : 02/04/2021

ACKNOWLEDGEMENTS

Thanks to Dr Tey Jing Yuen, the superviser of this thesis. This thesis was completed under his careful guidance. From the topic selection, simulation and theoretical analysis, Dr Tey gave me specific and detailed guidance. His profound professional knowledge and rigorous academic attitude have deeply influenced me and benefited me for life. Thanks again to Dr Tey for his serious guidance!

Finally, I want to express the deepest gratitude to the family who have supported and encouraged me for many years. Without the support of my parents, there would be no life today. I want to pay my highest respects to my parents!

DESIGN OF SCREW EXTRUDER FOR THREE-DIMENSIONAL CERAMIC PRINTING

ABSTRACT

3D printing is a rapid prototyping technology based on additive manufacturing. It uses plastics, ceramics, metals and other materials based on digital models to construct objects through layered printing and layer-by-layer stacking. This method has brought great innovation to the manufacturing field and is considered as a significant production tool for the third industrial revolution. And 3D printing technology has emerged as early as the 1980s. Because the technology was not mature at that time and the price was too expensive, it was not promoted and popularized. However, after more than 30 years' development, 3D printing technology has become more mature with more consumable prices, which creates favorable conditions for the popularization and use of this technology.

At present, 3D printing technology is relatively mature. In contrast, 3D ceramic material printing technology has less research and application. As known, ceramic materials have the advantages of high strength, hardness, temperature resistance and corrosion resistance, and high-tech ceramic materials with complex designs and fine structures have very important applications in the national economy and national defense fields. Nowadays, there are all kinds of methods for ceramic 3D printing, like light curing, Fused Deposition Modeling and inkjet printing. But the methods mentioned above have some drawbacks, which has the limitations on the ceramic 3D printing. So a proper method for ceramic 3D printing is very necessary. In this topic, the idea of designing a screw extrusion for ceramic 3D printing will be come up with.

As the key of this method, the slurry extrusion device is so critical that it has a crucial impact on the molding accuracy and printing efficiency of the printed product. Therefore, the design of a ceramic 3D printer slurry extrusion device with a reasonable structure is the key to study ceramic 3D printing technology. So the design and improvement of screw extruder has been developed in this topic. And by the use of CAD, the models and parameters of components of screw extruder designed such as motor, screw, hopper, barrel and hopper can be exactly determined and after designing, by the use of CAE, the printing performance of screw designed will be developed, such as pressure of ceramic slurry and screw, temperature distribution and printing speed of screw.

TABLE OF CONTENTS

LIST OF TABLES

LIST OF FIGURES

CHAPTER 1

INTRODUCTION

1.1 General Introduction

As one of the three pillars of today's social development, materials are the basis for human society to survive, and at the same time it plays a foundation and guiding role for the development of high-tech. With the rapid development of human society and the acceleration of economic globalization, a large number of high-tech products have continuously emerged on the market, the pace of updating new materials has been accelerating, and the technological era of material-led innovation has arrived. In order to gain a place in the fiercely competitive society, most companies will not hesitate to invest a large number of manpower and material resources in order to achieve greater breakthroughs in the technology, process and application of new materials in the various technical fields. In the history of material development, ceramic materials are one of the oldest materials manufactured by mankind. (Jin Zhihao, 2000) In the context of the development of ceramic molding technology and raw materials, ceramic materials have achieved rapid development from traditional ceramics which are generally made from rocks, minerals and clay, to the new ceramics made from artificially synthesized high-purity inorganic compounds. New ceramic materials, due to their stable chemical properties which are high hardness,

strength, temperature resistance, corrosion resistance and wear resistance, as well as special optical, electrical, magnetic, acoustic, thermal and sensitive properties, are widely active in the area of aerospace, national defense, machinery, electronics, chemical engineering, medicine, and construction hygiene. (Guan Zhenduo, 2011)

3D printing technology is a new kind of manufacturing technology which is speedily developing in the manufacturing field. Compared with traditional preparation methods, in the process of 3D printing and preparing parts, the computer controls the 3D printer to directly generate objects of any shape without any molds, which greatly simplifies the manufacturing process and shortens the production cycle, at the same time it greatly improves efficiency and reduces production costs. So 3D printing technology is regarded as a forming technology with significance of the industrial revolution. (Berman B,2012)

The introduction of 3D printing into ceramic component manufacturing provides new probabilities for solving various problems like good surface quality and dimensional accuracy. The scientists Marcus and Sachs first reported the 3D printing of ceramics in the end of 20th century. So far, with the greatest developments in computer science and material science, 3D printing technology has been definitely developed for ceramic manufacturing. (Chen Zhangwei et al, 2019) As a general rule, 3D printing technology can be easily divided into slurry-based, powder-based and bulk solid-based method due to raw material form after pretreatment, which is shown in Table 1.1 below.

Table 1.1: Ceramic 3D printing technologies

Feedstock form	Ceramic 3D printing technology type	Abbreviation
Slurry-based	Stereolithography	SL
	Digital light processing	DLP
	Two-photon polymerisation	TPP
	Inkjet printing	IJP
	Direct ink writing	DIW
	Three-dimensional printing	3DP
Powder-based	Selective laser sintering	SLS
	Selective laser melting	SLM
Bulk solid-based	Laminated object manufacturing	LOM
	Fused deposition modelling	FDM

Nowadays, ceramic 3D printing is widely used in the areas of aerospace, medical science and industrial manufacturing. For instance, the flexural strength of 3D printed alumina ceramic sintered products can reach 300Mpa and the Mohs hardness can reach 9, coupled with excellent wear resistance and good high temperature resistance. Ceramic precision parts are widely used in occasions where there are special requirements for wear resistance, hardness, and high temperature. (Liu Houcai et al, 2008)

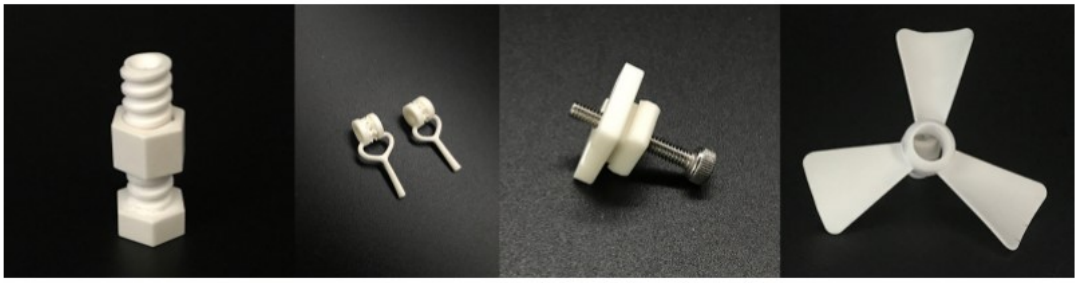

Figure 1.2: Nut, Jewelry core, Bolt and Fan blade made by 3d ceramic printing

With continuous breakthroughs in aerospace technology, the development of aerospace vehicles is coming into the stage of high temperature, high altitude, and high speed bit by bit. Lots of aerospace sensors need to work in extremely harsh actual working environments which are severe vibration, high temperature, high pressure, and corrosiveness as the examples. It causes that the production of sensors will face great challenges and difficulties. In order to insulate and fix the sensitive components and conductive lines in the sensor, a bushing is usually added to the metal shell. Due to the limitation of the processing technology, the bushings are all polymer injection parts used before. As the temperature rises and insulation performance requirements increase, polymer materials are difficult to meet the harsh working environment requirements.

Ceramic materials have great characteristics like high compressive strength, temperature resistance, and corrosion resistance, and they are regarded as the poor electrical and thermal conductors. They are the best choice for manufacturing the aerospace sensor bushing. However, the aerospace sensor bushing has a small size with high precision and complex shape. If using the traditional method to prepare the aerospace sensor bushing, the cost will be high with the complicated process and the long development cycle. To solve this problem, the researchers from the company iLaser utilized the method of ceramic laser printing to produce the aerospace sensor bushing which met the requirements of smooth surface and stable insulation performance. (Liu Houcai et al, 2008)

The ceramic 3d printing is also widely active in the field of medical science. The ceramic material used in this area includes bio-inert ceramics like Alumina ceramic, Zirconia ceramic and Silicon Nitride ceramic, and bio-active ceramic such as Hydroxyapatite ceramic and Tricalcium Phosphate ceramic. Alumina, zirconia and silicon nitride ceramic materials usually can not be easily degraded, they have high

wear resistance and biocompatibility, so they can be used to make long-lasting implantable medical devices, such as artificial caput femoris, acetabular cup lining and dentures.

The ceramic material used in 3D printed dentures is usually zirconia, which is processed by digital scanning and modeling to the dental cast, three-dimensional design, 3D printing, degreasing and sintering, and glazing. In China, some companies have used ceramic 3D printing technology to produce zirconia ceramic dentures that have undergone mechanical and biological tests, and obtained marketing approval. The zirconia denture has high precision and permeability. (Manicone, 2007)

Silicon nitride has very high fracture toughness and it is a super hard ceramic material. A US biomaterials company took the lead in the world to develop medical silicon nitride materials. The company used the 3D printing technology of automatic grouting to manufacture the complex silicon nitride Spine Fusion Implant and verified its performance, confirming that 3D printed silicon nitride implants have certain property of corrosion resistance in the human bone, which meets the requirement of manufacturing implants. (Chen Li, 2002)

The chemical composition of tricalcium phosphate and Hydroxyapatite is similar to the component of bone, which has good biocompatibility, osteoinductivity, osteoconductivity, and degradability. In China, a medical team from the National Additive Manufacturing Innovation Center used Stereolithography Apparatus, digital light processing, selective laser sintering and melting, and inkjet printing to create movable artificial eyes with complex structures, and they opened up a new chapter in the application of ceramic 3D printing technology in the field of personalized medicine. In the future, more new processes and new materials will be applied to the medical field, bringing new treatment options to patients. (Zhang Wenyan, 2013)

At the same time, the commercialization of ceramic 3D printing technology has to overcome the difficulties like manufacturing speed, material properties of products, machine and material costs, printing accuracy and quality. There are some issues like how to effectively accumulate ceramic objects with accurate size and complex structure, how to decrease the residual stress in the sintered body during sintering, and how to prepare more stable ceramic inks, which the scientists have to face and solve. (Liu Wei et al, 2017)

The ceramic extrusion process is one of the steps for ceramic 3D printing. It is similar to the FDM process of plastic materials. They both extrude the materials and stack them layer by layer on the platform, and finally print and shape according to the designed model. However, the mass production of ceramic hot-melt filamentary materials is not mature enough, and the performance is not stable enough by using FDM technology. (Wang Di et al, 2011)

The extruder is a critical part of the additive manufacturing process based on extrusion. The structure design of the extruder and the selection of the extrusion method are directly related to the smooth progress of the forming process and the quality of the ceramic parts. The extrusion methods of the extruder are divided into screw extrusion, pneumatic extrusion and plunger extrusion. Screw extrusion is the process of extruding ceramic slurry or paste through the shearing force of a rotating screw. The biggest advantage of screw extrusion is that it can realize continuous feeding of materials. (Harold F. Giles et al, 2004) So combining the technology of FDM with the screw extrusion, a new method of ceramic printing is proposed, which will overcome the difficulties in FDM. In the process of ceramic 3D printing, the ceramic 3D printer slurry extrusion device plays an important role. An extruder with the proper structures will benefit for the reliability and efficiency of the extrusion of ceramic slurry, which is also the purpose in this project.

1.2 Importance of the Study

This project will focus on a novel approach to design and develop a compact single screw extruder for ceramic 3D printing. It will overcome many drawbacks of the other ceramic printings, which are the high cost, the tough requirements, occurring many issues after the ceramic printing. By using the single screw extruder for extrusion, it will expand the flexibility and capability of a 3D printer.

1.3 Problem Statement

At present, powder injection molding which is an advanced molding technology, is developing at a rapid rate of 22% annually at home and abroad, and the injection molding of ceramic materials has also been applied in some fields. (Li Xinjun et al, 1999) But there exists an issue that the particle size distribution, specific surface area, particle size and particle shape of the ceramic powder used in ceramic injection molding have a significant impact on the entire process, which means that ceramic injection molding has special requirements for the properties of the powder. (G Bandyopadhyay et al, 1994)

The research has shown that due to the addition of a large amount of binder in ceramic injection molding, the size shrinkage after sintering is much greater than that in compression molding. In order to prevent the problems of deformation and decrease in dimensional accuracy, it is important to raise the powder loading, and reduce the shrinkage of the product in ceramic injection molding, which means that ceramic powders with extreme obturation density should be used in ceramic

injection molding. For the shape of the powder, spherical powder is more ideal, but the meshing force between the spherical powders is poor during the degreasing process, and there is a risk of deformation. If selecting the powder with the irregular shape, there will be an agglomeration caused by the friction between the powder particles, which will affect the full mixing between the powder and the binder, and reduce the powder loading at the same time. And another issue is that there may be a high initial tooling and machinery cost for injection moulding. (R M German et al, 1992)

Compared with ceramic injection molding, the ceramic 3d printing has some advantages which are that there is no need for the molds during the manufacturing process and ceramic 3D printing does not require a centralized and fixed manufacturing workshop, which reduces production procedures and greatly saves production costs. (Cong riyuan et al, 2019) Therefore, it is so popular that it has been extensively used in the area of ceramic preparation at the moment. But there are some drawbacks in the methods of ceramic 3D printing, which are shown below as the examples. At early stage, researchers GRIFFITH M L et al (1996) used Stereo Lithography process to make alumina ceramic parts, and used photosensitive resin to configure photosensitive alumina ceramic slurry during the experiment. However, the study showed that the photosensitive resin used in the experiment was expensive, it had extremely high environmental requirements, and it was not conducive to long-term storage. The most important point was that the material was toxic, not only harmful to humans, but also polluting the environment. Therefore, the application in the field of ceramic preparation is limited. Another group of researchers used alumina powder as the raw material and mixed polymers as the binder to prepare alumina ceramic bodies through Selective Laser Sintering, and then debinded and sintered to obtain ceramic parts. However, the ceramic parts manufactured by this method were loose and porous, they had low bending strength and poor product performance, which basically did not meet the current requirements for ceramic products. (Subramanian

K et al, 1995) Xu uses the technology of FMD to prepare alumina ceramics. Although it is simple to operate, low energy consumption, and low cost with no pollution to the environment, the materials used in this technology are mostly thermoplastic polymers, which are under research in ceramic printing and forming. (Liu K et al, 2017) Therefor, it is critical to choose a more proper method for ceramic 3D printing, relatively.

1.4 Aim and Objectives

The aim in this project will cover with two parts which are designing a compact single screw extruder and simulating the performance of the single screw for ceramic feedstock which is showed as follows:

1. Design a compact single screw extruder
2. Determine the performance of single screw through finite element analysis

1.5 Scope and Limitation of the Study

The study will focus on the design of a compact screw extruder for ceramic 3D printing. The scope will refer to screw based extrusion methods with its simulation and the limitation will be limited to ceramic powder formulation which is used in extrusion forming. In this project, the ceramic material which will be chose is limited to the Alumina ceramic.

CHAPTER 2

LITERATURE REVIEW

2.1 3D Printing Technology

3D printing manufacturing technology is based on the principle of stacking and forming discrete materials layer by layer. And it utilizes the way of accumulating materials layer by layer to produce solid parts by design data of CAD. Compared with conventional material removal (cutting) technology, it is regarded as a way of "top-down" material accumulation manufacturing. The 3D printing manufacturing technology has solved many the problems which was difficult to manufacture the forms of parts with complex structures in the past. And it also greatly reduces the processing procedures and shortens the processing cycle. Nowadays, 3D printing ceramic mainly includes ink-jet printing (IJP), Stereolithography apparatus (SLA) and Selective laser sintering (SLS) and fused deposition modeling (FDM). These technologies can be classified according to different standards. Among them, laser forming methods include SLA, SLS and LOM, and the other two are non-laser forming methods. There are FDM and SLS technologies that require support structures, while the other three do not require support structures. Finally, according to the process, it can be divided into direct forming and layer-by-layer bonding. IJP technology is to mix ceramic powder and binder to prepare ceramic ink, which is

directly formed by 3D printing. So it belongs to the direct forming. The method of other 4 technologies is the layer-by-layer bonding. (Ben Yue, 2016) The table 2.1 shows the comparison of each technology in terms of raw materials and finished product scale.

Table 2.1: Comparison of 3D printing technologies

	IJP	FDM	SLA	LOM	SLS
Raw materials	Ceramic inks	Filamentous materials	Mixture of ceramic and photosensitive resin	Thin-film materials	Powders
Size	Small scale	Large scale	Small scale	Large scale	Large scale
Costs	Low cost	Low cost	Higher cost	Higher cost	Higher cost
Complexity	Complex	Complex	Complex	Simple	Complex
Support structure	Not required	Required	Required	Not required	Not required
Two cure processes	Not required	Not required	Required	Not required	Not required
Laser technology	Not required	Not required	Required	Required	Required

In this part, the principles and characteristics of four methods mentioned above for ceramic printing will be cover, which include ink-jet printing (IJP), Stereolithography apparatus (SLA) and Selective laser sintering (SLS) and fused deposition modeling (FDM). On the one hand, for the first three methods, the aim is just to do a shallow review because the printing method and principle described in this article are completely different from those of three. On the other hand, the last method fused deposition modeling (FDM) has some same characteristics as the method which is the screw extrusion based ceramic 3d printing used in this project. So the review of the method fused deposition modeling (FDM) will be more detailed.

2.1.1 Inkjet Printing

The origin of 3D printing ceramic technology is the inkjet printing. The main raw material of this technology is "ceramic ink", and no supporting structure is required during the printing process. Inkjet printing technology itself can be separated into

solid inkjet and liquid inkjet due to its theory, and liquid inkjet printing technology can be separated into the bubble type and the piezoelectric crystal chip type. As the bubbles expand and reach a critical value to overcome the surface tension of the ink, the ink is ejected from the top of the nozzle capillary. The ceramic ink is controlled to draw patterns according to the computer's pre-modeled data, and the superimposition of layers realizes the 3D printing process. After the heating is stopped, the ink is cooled, then the bubbles begin to condense and shrink, and the ceramic ink will retract, finally the supply of ceramic ink will stop. (Chia H W et al, 2015) With 3D inkjet printing technology, users can design personalized ceramics according to their needs, greatly reducing the cost and saving manpower and material resources. This technology does not require the assistance of laser technology, so the cost is low, and it has been widely developed and applied in daily life.

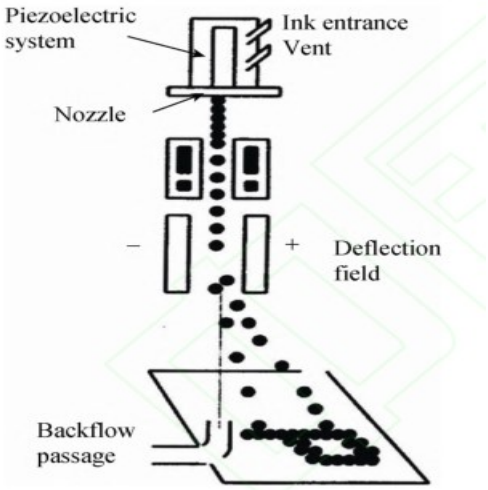

Figure 2.1: Schematic illustration of the IJP technique

For the use of the technology of IJP for ceramic comconent printing, it was recorded in the book writen by Blazdell et al in 1995. In his experiment, they found that low volumne fractions could cause a long drying time by using Zinc Oxide and Titanium Oxide ceramic inks which have the volume fractions lower than 5 vol%.

But they only got the simple multilayer structures with poor surface quality. After that, Blazdell et al printed a small columnar array based on 14 vol% of submicron zinc oxide particles in the ink with great success. Then, the team successfully printed a small columnar array based on 14% (volume) of submicron zinc oxide particles in the ink. They found the significant effect of different ink characteristics, especially viscosity and surface tension on printing behavior. By the experiemnt of making an 40 vol% alumina loading utilizing ceramic ink, Seerden found that the ceramc parts had a small feature size which was only lower than 100μm.

At present, there are two main factors restricting the development of 3D ceramic inkjet printing technology, which are the configuration of the ceramic ink, and the clogging of the inkjet print head. On the one hand, ceramic ink is generally composed of inorganic non-metallic materials, dispersants, binders, surfactants and other series of auxiliary materials. The basic requirement of this kind of ink is that the particles of inorganic non-metallic materials must be less than 1μm, the particles must be evenly distributed and there is no agglomeration between particles. However, since the ink in 3D ceramic inkjet printing technology needs to undergo high temperature vaporization, the chemical properties of the ink are easy to change and unstable. During the jetting process, the ink's micro-directivity and shape cannot be precisely controlled, which affects the printing accuracy and quality. (Rutz A L et al, 2015) On the other hand, regarding to issue of clogging of the inkjet print head, whether it is reducing the viscosity of the ceramic ink or increasing the diameter of the nozzle capillary tube, the printing effect will be greatly reduced, and the accuracy of the finished product will be reduced. (Isakov D V et al, 2016) These two problems need to be solved urgently in future development.

2.1.2 Stereolithography Apparatus

Stereolithography apparatus (SLA) is to use a laser with a specific wavelength and intensity to gather in the surface of the photocured material, so that it solidifies from point to line, from line to surface, and then completes a layer of drawing operation. After that, the lifting platform moves one-layer height in the vertical direction, and then solidify another layer. By this method, the layers will form a three-dimensional entity. (HUANG M J et al, 2017) The research from University of Michigan in the United States first proposed to combine Stereolithography apparatus with ceramic material preparation technology. The material used in Stereolithography apparatus technology is a slurry which is a blend of photosensitive resin and ceramic powder. (GRIFFITH M L et al, 1996)

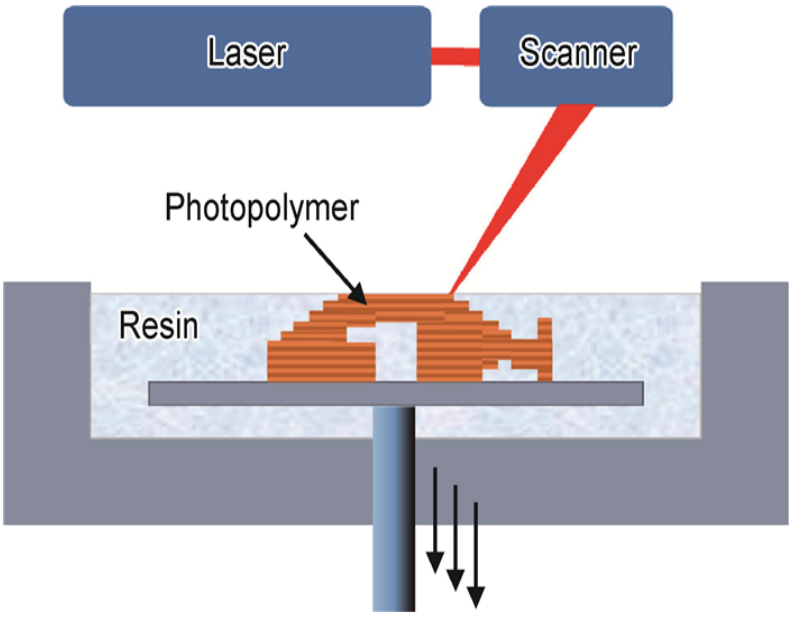

Figure 2.2: Schematic diagram of SLA light curing process

The development of Stereolithography apparatus (SLA) has been relatively mature and it is fit to the production of parts with complex structures and high precision requirements. Besides, the technology can realize online operation and remote control, which contribute to the full automation of production. (Ma X L,

2013) European companies have developed Stereolithography apparatus 3D printing equipment, which has greatly improved the forming accuracy and speed, and the surface finish of parts. Secondly, because this technology does not require sintering or the addition of sintering agents, it can be completed at a lower temperature and pressure, and the finished product has better thermal and mechanical properties. (Zhang K S et al, 2015)

There are many researches on the Stereolithography apparatus for ceramics. The study on the influence of alumina ceramic slurry on light transmittance shows that light can reach the back of each layer with the existence of ceramic particles, and the transmittance of direct light is basically zero, and the transmitted light is dispersed. (M. Kurimoto et al, 2016) The research on the effect of ceramic particle size and solid content on curing width and curing depth shows that the curing width and curing depth increase with the ascent of particles, and the curing width decreases with the increase of the solid content, but the curing depth increases with the ascent of the solid content, and the curing width will be significantly larger than curing depth. (M. Kurimoto et al, 2016) The researcher Eckel developed a kind of new photosensitive resin containing the Silicon carbide material. He produced large parts by this technology used in the areas of sensors and aerospace because of the Silicon carbide's characteristics of high strength and high temperature resistance. (Yang K et al, 2020)

However, the shortcomings of Stereolithography apparatus technology are also obvious. One the one hand, the ceramic-photosensitive resin mixed liquid currently used in this technology is a toxic and irritating material and it needs to be stored away from light. Therefore, when using 3D printers by this method, it is necessary to ensure the circulation of air and dim light in the working environment. The requirements are harsh for conducting scientific research experiments with high cost, and its printing efficiency needs to be further improved. On the other hand, the

realization of this technology also needs to found a support structure. The post-processing should consider the secondary curing of the formed parts and the support structure needs to be removed in the end, which is more complicated. (SPOATH S et al, 2014)

2.1.3 Selective Laser Sintering

Selective laser sintering (SLS) is an additive manufacturing (AM) technology, which utilize a laser as a power source to sinter powder materials (usually nylon or polyamide), and aligns the laser at a point of itself in space defined by the 3D model. And the materials are bound together to form a solid structure. In the process of Selective Laser Sintering (SLS) for ceramic printing, which is shown in Figure 2.5, the ceramic is first wrapped and spread out with a thermoplastic polymer material, and then a high-energy laser is used to scan the powder in a certain part. The working principle is that the temperature of the powder rises sharply and then melts and mutual bonds under the action of the laser beam. And then after leaving the laser scanning, it quickly cooled and solidified. By repeating the above operations, new powders can be spread layer by layer and solidified to finally obtain ceramic embryos, which are then fired at high temperature after degreasing treatment to obtain ceramic devices. (WILKES J et al,2013)

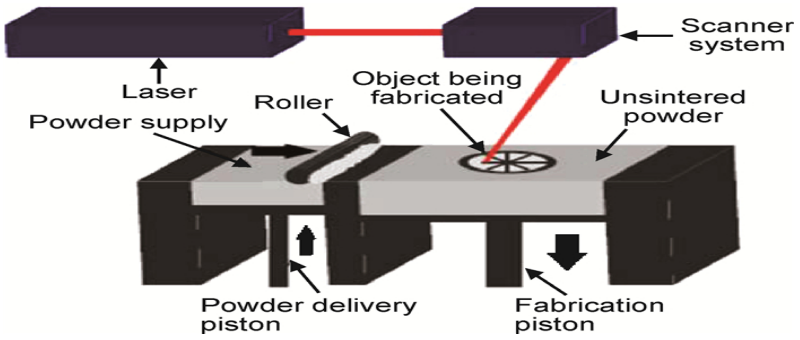

Figure 2.3: Selective Laser Sintering

There are many outcomes from the study on the Selective Laser Sintering for ceramics. Researcher Exner created a Q-switched pulsed laser system with a wavelength of 532 nm in order to study in laser micro-sintering of silica-alumina (SiO2/Al2O3) powder. During his experiment, he utilized a fine powder with the small particle size which is less than 1 μm. The result showed that the ceramic parts had the geometric resolution with high value and excellent surface quality. After heat treatment, pores and microcracks are reduced, and the tensile strength reached 120 MPa, which could not be used in high-strength components because the tensile strength obtained was still very low. (Exner et al., 2008) In biomedical area, Liu utilized the direct laser sintering to prepare bone scaffolds on a blend of hydroxyapatite (HA) and silica slurry. By the simulation to the process of laser sintering ceramic. Tian concluded that the laser scan strategy could affect the residual stress distribution and sintering temperature. (Tian et al, 2012)

The importance of SLS technology is the material printed, but the development of SLS technology is not yet mature (WU Q et al, 2015). At present, the main materials used are carbides, oxides, and nitrides (ONUH S O et al, 1999). The content and types of organic materials used as binders in the materials directly affect the density and mechanical properties of the ceramic body. The matching of the output energy of the laser beam and the printing material plays a decisive role in the forming accuracy, the structure of the processed part and the mechanical properties. The main advantages of SLS technology are high forming efficiency, material utilization with low price. SLS technology uses laser beams to sinter ceramic materials, which has higher requirements on the working environment and facilities for printing. The preheating system and thermal insulation system required for the sintered ceramic body during the printing process are also problems that the SLS technology urgently needs to solve. And at the same time, there will be poisonous gas and dust generated during the molding process which pollute the environment. (JI Hong-chao et al, 2018)

2.1.4 Fused Deposition Modeling

The process of Fused deposition modeling is to heat and melt various hot-melt filamentous materials, which is a kind of 3D printing technology. It is also known as Fused Filament Modeling (FFM). The temperature of the hot melt material is always slightly higher than the solidification temperature, while the temperature of the formed part is slightly lower than the solidification temperature. After extruding the hot melt material from the nozzle, it is fused with the upper layer. After the deposition of a layer is completed, the workbench is reduced by a predetermined increment by a layer of thickness, and then the melt-blown deposition is continued until the entire solid part is finished. (Zhao Guifan et al, 2008)

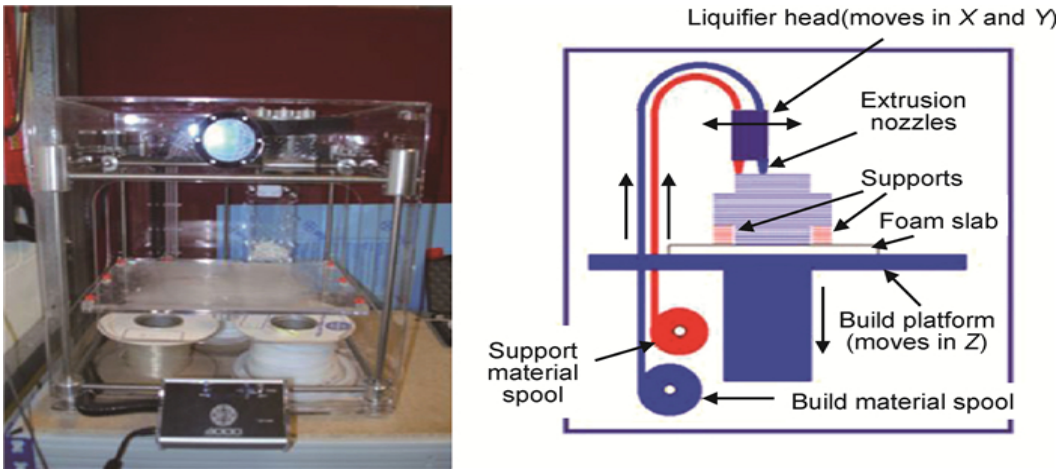

Figure 2.4: Fused Deposition Modeling

Fused Deposition of Ceramic (FDC) is an improved FDM process in which thermoplastic filaments filled with ceramic powder are extruded through the FDM. During the fused deposition of ceramics, the thermoplastic polymer will melt and carry the ceramic powder. The green ceramic parts have about 40-45% binder like injection-molded parts. And then, the process is debind and sinter the parts in cycles for densification. The process development of FDC needs to optimize the composition

of the thermoplastic binder, filament manufacturing, the burn-out of FDC and binder, and the development of the sintering cycle. (Seyi Onagoruwa etal, 2001)

The study on the formulation of ceramic materials for extrusion freeform fabrication (EFF) and fused deposition of ceramics (FDC) show that The rheological characteristics and extrusion pressure of the paste are very sensitive to the volume fraction of solids. The change of die entry extrusion pressure with solid content obeys the same trend as that given by the Krieger-Dougherty equation. For the change of die land extrusion flow behavior with solid content, it can be concluded that when the two-roll milled slurry with solid content is less than 54% v/v, the ceramic slurry will perfom less slip flow. When pastes with a solids content reaches 53/54% v/v and is lower than the critical solids content of 56/57% v/v, the apparent shear viscosity of the paste will behave as independence to the solid loading. (Powell J et al, 2013)

R.Vaidyanathan with assistants designed and installed an extrusion head on the basis of Stratasys' FMD printer, and used ceramic materials including silicon nitride, alumina and zirconia to realize the extrusion of ceramic materials. (R. Vaidyanathan et al, 2000) Research on the extrusion of ceramics through fine nozzles has indicated that highly filled ceramic suspensions can be extruded through the nozzles which have the diameter less than 100mm. The smallest sapphire nozzle can be 76 mm and operated continuously. The application of twin-screw extruder with a high-shear cannot offer a suspension, which will continuously pass through a nozzle with a diameter of less than 510 mm. (Imen Grida et al, 2003)

Jie Li did a research on the effect of temperature on the extrusion of ceramic materials through experiments, and designed and manufactured a gantry-type 3D printer with an extrusion mechanism shown in the Figure 2.5 for alumina slurry forming, the relative density and mechanical properties of each part after sintering

are compared. The results show that the relative density, flexural modulus and flexural strength of ceramic parts manufactured at 40°C are 96.73%, 311 GPa and 338 MPa, respectively. The relative density, flexural modulus and flexural strength of parts manufactured at -20°C are 91.55%, 280 GPa and 300 MPa, respectively. At 40°C, when the bottom diameter is 38 mm, the minimum deposition angle is 50°C; at -20°C, when the bottom diameter is the same, the minimum deposition angle is 28°C. Both of the test rods which are manufactured at 40°C and -20°C, relatively have great flexural strength and relative density. For the rods manufactured at 40°C, it behaves higher mechanical characterisitcs. The minimum deposition angle of the hollow cone manufactured at -20°C is smaller than that of the hollow cone manufactured at 40°C, which indicates that the frozen environment has a greater capacity to manufacture larger and more complicated hollow cones with no use of supporting (sacrificial) materials. (Jie Li et al, 2015)

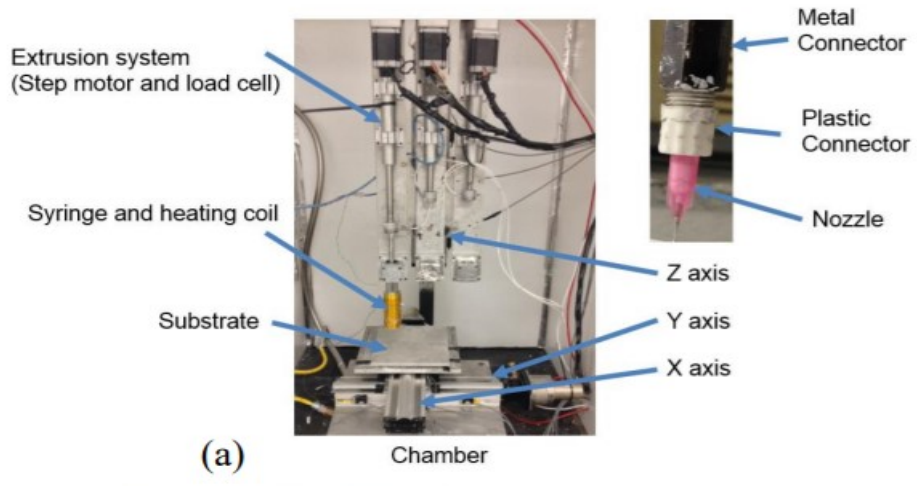

Figure 2.5: The 3D printer in Missouri University of Science and Technology

The technology of Fused Deposition Modeling does not require the assistance of laser technology, so the cost is lower and the later maintenance is also more convenient. However, this technology requires a supporting structure because the height increases during the printing process of stacking layers, and the lower layer

material cannot fasten the weight of the upper layer material. Especially when printing more complicated originals, the location and shape of the upper layer outline are significantly different from those of the lower layer. So it is important to establish a support structure outside to make sure that the ceramic parts can not collapse during the printing process. (Carneiro O S et al, 2015)

The realization principle of the Fused Deposition Modeling technology is simple, but the temperature at the nozzle is high during the 3D printing process, and the requirements for the raw materials are higher. In order to meet the forming requirements, in addition to forming filamentary materials, the raw materials must have the properties of bending strength, compressive strength, tensile strength and hardness. In addition, the filamentous ceramic material must have a certain degree of fluidity and consistency after the heating and melting processes at the nozzle, and the shrinkage rate cannot be very large, otherwise the parts will be deformed. (McNulty T F et al, 1998) Therefore, the types of filamentous ceramic materials used in the fused deposition modeling technology are greatly restricted, so this technique usd in ceramic 3d printing is not very mature and further study need to be done.

2.2 The Research to Slurry Extrusion Device

Existing ceramic 3D printers use a syringe-based mechanism to achieve ceramic 3D printing. But the syringe based mechanism has a drawback of intermittency or discontinuity during printing. The research shows (M. Venkatesan et al, 2019) that if the syringe barrel is loaded with the feed material in the form of paste or semi-solid. Once the stock material is fully extruded then the printer will has to be stopped for refilling the feed material. So such extruding system is not suitable for printing the objects with large dimensions. In order to deal with it, screw feeding concept is

implemented for continuous extrusion of ceramic. Screw extruders are commonly used in polymer based 3D printing, it is also called as pelletized extruder. In the case of Fused Deposition Modelling “Buckling” is a problem with feeding the material in the form of filament. To overcome that screw extruders are introduced. Here the rotation of screw aids the homogenous delivery of material. Typically a pelletized screw extruder consists of feeding hopper, screw (rotating), barrel, nozzle and a heater. The continuous rotation of the screw is aided by the motion subsystem. Screw extrusion offers better rheology control than the syringe extrusion system.

The working principle of the screw extruder is that the pellets are usually kept in a hopper and fed into the extruder through the entrance of hopper. Then they flow directly into the spiral channel, and then are conveyed to the nozzle through the spiral. A heat block near the nozzle heats the barrel and screw, so that it can liquefy the polymer during the conveying the pellets. Once the pellets are liquefied and leaves the spiral channel, the pellets will enter the buffer chamber. The buffer chamber is referred to the empty space between the bottom of the auger and the nozzle. Relying on the rotation of the motor, the pellets are compressed in the buffer chamber and forced to pass through the small hole at nozzle. (Dylan T.J. Drotman et al, 2015)

The flow can be usually divided into geometric areas called partially and fully filled zones in the extruder. The partially filled area is the transport zone of materials and exposed to air pressure. And the fully filled zone has the capacity of melting. (Dylan T.J. Drotman et al, 2015)

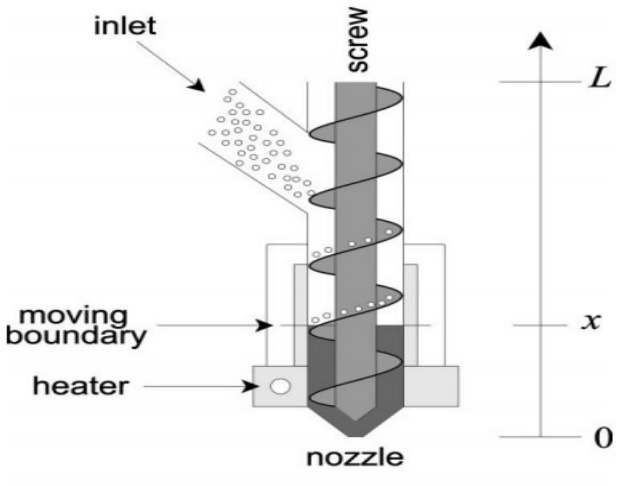

Figure 2.6: The screw extrusion process

2.3 The Review to Extruder Screw

The screw is the heart and the important part of the extruder. The performance of the screw determines such as productivity, plasticization quality, dispersion of additives, and melt temperature of an extruder. In this part, the review will cover the sections, diameter, the clearance and Helix Angle of the screw.

2.3.1 The Three Sections of Extruder Screw

The first part is the feeding part, where the material contacts the screw. When the screw rotates, it transports the material to the other end. In order to regulate the feeding of materials, there are multiple scrapers with constant channel depth and the conveying part also has a deeper channel depth to convey more material to the subsequent part.

The second part is the compression part. It can be seen from Figure 2.8 that

the depth of the screw channel gradually decreases throughout the screw, resulting in a compression effect. By compressing the melt and material, the air can be removed from the melt and voids in the melt can be prevented. In addition, by reducing the depth of the screw, the melt is exposed to more heat to melt the remaining thermoplastic pellets or powder. As the thickness of the melt decreases, the surface area of the extruder barrel exposed to heating increases, thereby heating the melt more uniformly.

The last part is the metering part. In the metering section, the depth of the channel is the shallowest to increase the pressure to extrude the thermoplastic. The accumulated pressure will determine the extrusion rate of the thermoplastic. (Syed Ali Ashter, 2013)

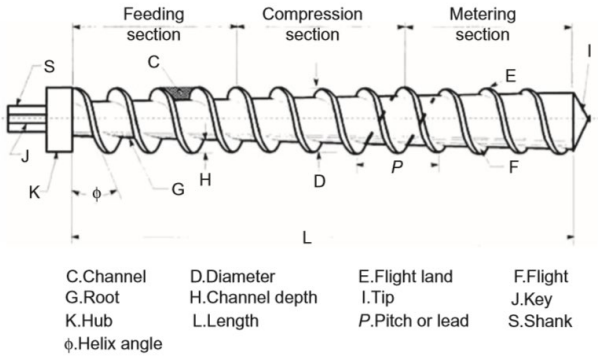

Figure 2.7: A typical screw design

2.3.2 The Diameter of Screw

As the diameter of the screw ascends, the processing ability of the extruder increases accordingly. The productivity of the extruder is proportional to the square of the screw diameter D. The ratio of the effective length to the diameter of the working part of the screw (called the ratio of length to diameter, expressed as L/D) is usually 10 to 30. If the value of L/D is large, it will improve materials' temperature

distribution, which will facilitate the mixing of material, and will reduce leakage and reverse flow at the same time. but the L/D can not be too large, because self-weight of the screw will increase, which easily cause scratches between the material and the screw, and lead to more difficult manufacturing and processing. In addition, the power consumption of the extruder will also increase. (Dylan T.J. Drotman et al, 2015)

2.3.3 The Clearance

The half of the gap between the inner diameter of the barrel and the diameter of the screw is named as the clearance δ, which can influences the production capacity of the extruder. As δ rises, the productivity will decrease. Usually it is appropriate to control δ at about 0.1-0.6 mm. If δ is small, the shearing effect of the material is greater, which contributes to plasticization. However, if δ is too small, the high shearing effect will cause the thermo-mechanical degradation of materials, and at the same time, it is easy for the screw to rubbed against the barrel wall. For ceramic 3d printing, the design for the clearance will be set at 2% of the diameter for screws. (Dhinesh K S et al, 2019)

2.3.4 The Helix Angle of Screw

The helix angle Φ is the angle between the screw thread and the cross section of the screw. As Φ ascends, the production capacity of the extruder will increase. Usually the helix angle has a range from 15° to 45° and changes along the direction of the screw length. The equidistant screw is widely used that it usually takes the pitch equal to the diameter, so that the clearance Φ can be calculated which is about 17.6°. (Dylan T.J. Drotman et al, 2015)

2.4 The Review of Other Components of a Screw Extruder

Hopper is the cylinder through which the material is fed into the barrel. Since the angle of descent is very critical with regard to the work to be done to force the material down the hopper, it is desirable to have a hopper angle greater than 45° (with respect to horizontal).

Barrel is the cylinder which houses the screw and constitutes the main body of the extruder. The barrel should be of study construction and should be made of a material which can resist the wear that could be caused by the feed material.

The nozzle is the part which is responsible for the flow of material at the desired size. Its design should aid in the process of achieving constant flow velocity at the outlet and there should be enough pressure buildup in the nozzle region to have continuous extrusion. (Dylan T.J. Drotman et al, 2015)

2.5 The Optimization of Screw Extruder

2.5.1 Printing Accuracy

To improve the printing accuracy, the diameter of the nozzle of the screw extruder is required to reduces to 0.5mm. By the simulation of the outlet flow rate of the screw extruder in the stop-start state, it is shown that the nozzle diameter reduces from 0.6 mm to 0.5 mm, the highest average flow velocity at the outlet decreases from 10.81 mm/s to 7.40 mm/s with a decrease of 31.54%. The printing speed of the application

and printing efficiency also decrease. On the other hand, the printing accuracy can be further improved when reducing the diameter of the nozzle to 0.4 mm, but in the test, the nozzle is easily clogged, and the cleaning requirements of the extrusion device after the printing experiment are greatly improved with the increase of the cost. (LI Yaogang et al, 2019)

2.5.2 Outlet Flow Rate

Increasing the screw speed can increase the internal pressure of the screw extruder and the outlet flow rate. When increasing the screw speed to 50 r/min, the result shows that the outlet flow rate is increased to 8.90 mm/s. When the speed is increased to 60 r/min, the outlet flow rate can increase to 11.04 mm/s.

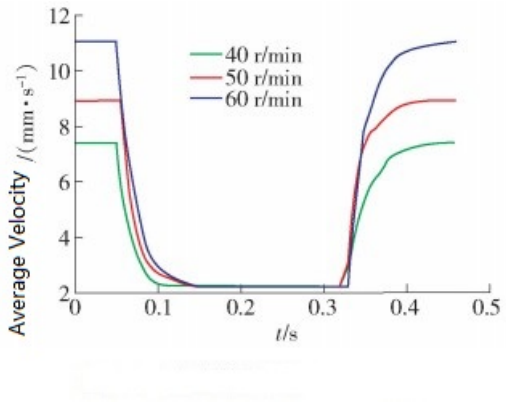

Figure 2.8: Average outlet flow rate at different speeds

Changing the size of the gap between the outer diameter of the screw and the inner wall of the barrel will also have a greater impact on the outlet flow rate. Figure 2.10 shows that when the gap increases from 0.50 mm to 0.75 mm, the average outlet flow rate can only reach 5.01 mm / s; When the gap is reduced to 0.25 mm, the average outlet flow rate can increase to 10.68 mm / s. It can be seen that reducing the gap between the outer diameter of the screw and the inner wall of the barrel can

increase the outlet flow rate and improve the printing efficiency. On the other hand, the smaller the clearance on the inner wall of the barrel is, the less slowly the outlet flow rate will decrease when the screw stops. And the faster the outlet flow rate increases when the screw resumes rotation, which shows that the clearance can play a role in releasing the internal pressure of the screw extrusion device. (LI Yaogang et al, 2019)

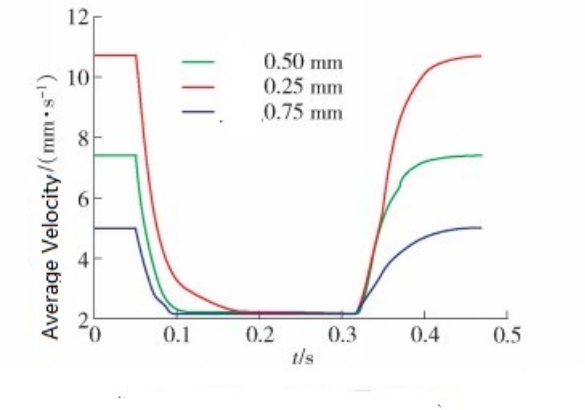

Figure 2.9: Average outlet flow rate at different gaps

By changing the pitch and length of the screw, it is showed that by increasing the variable pitch section of the screw, a greater pressure will be provided for the internal material of the screw extruder to increase the outlet flow rate. When the length of the variable pitch section of the screw is set as 10 mm, and the screw groove depth is changed from 12 mm to 24 mm. By changing the screw groove depth to 3 mm and 1 mm respectively for research. The results shows that changing these two factors does not have a positive effect on the improvement of the outlet flow rate, so the impact of these two parameters on printing is ignored, and the original parameters remain unchanged. (LI Yaogang et al, 2019)

Integrating the optimization results, the nozzle diameter of the screw extrusion device is changed to 0.5 mm, the speed increases to 60 r/min, and the gap between the outer diameter of the screw and the inner wall of the barrel reduces to

0.25 mm for simulation analysis. The simulation results are shown in Figure 2.11, the maximum outlet flow rate can reach 15.07 mm/s, so the printing speed can be set to 15 mm/s, which achieves the optimization purpose of improving both printing quality and printing efficiency. (LI Yaogang et al, 2019)

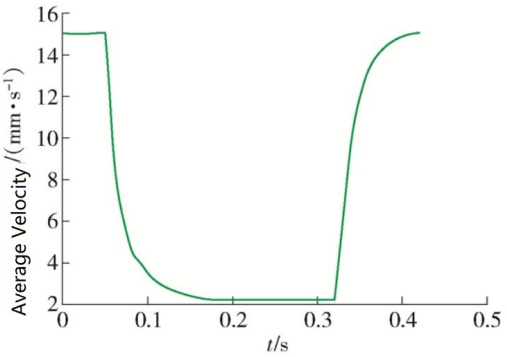

Figure 2.10: Outlet flow rate of optimized screw extrusion devicein the stop-start state

2.6 The Properties of Alumina Ceramic

Alumina ceramic is a ceramic material with α-Al2O3 as the main crystal phase, belonging to the trigonal crystal system, the structure is shown in Figure 2.11. As shown, Oxygen ion(O^{2-}) forms the most densely packed hexagon in the crystal structure, and Aluminum ion Al^{3+} is located on the eight sides surrounded by 6 oxygen ions. In the center of the body, the crystal structure is compact, which is the most stable crystal form among all kinds of forms of alumina. Its theoretical density is 3.98g/cm3 with Mons' hardness scale 9, the bending strength of alumina sintered products can reach 250 MPa, and the hot pressing products can reach 500 MPa, melting point is 2050℃. The theoretical permittivity of alumina ceramic material is 9~10.5 at 1 MHz, the specific volume resistance is greater than 1014 Ω·cm at 100°C,

and the thermal conductivity is 29 W/(m·k). Therefore, alumina ceramics have good mechanical properties, high temperature properties, electrical properties and chemical stability. (Zhang X F et al, 2010) The specific information is showing in Table 2-1 below.

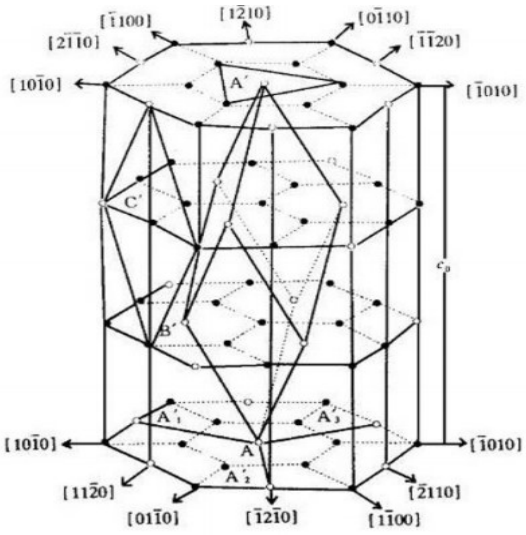

Figure 2.11: Crystal structure of α-Al2O3

Table 2.2: The properties of alumina ceramic

Properties	Applications
Mechanical properties	Mechanical precision parts, bearings, cutting materials
Insulation	Integrated circuit chip, spark plug
Conductivity	Na-S battery solid electrolyte, oxygen sensor
Optical performance	Laser material, high pressure sodium vapor light emitting
Chemical properties	Catalyst carrier, corrosion resistant material, solid enzyme
Biological performance	Artificial bone, artificial teeth
Thermal performance	High temperature resistant materials, thermal insulation

2.7 The Review of the Rheological Behavior of Alumina Ceramic

The relationship of fluid shear stress τ with the change of shear rate Ds is called rheological properties. According to different rheological properties, fluids can be

roughly divided into three types: pure viscous fluids, viscoelastic fluids and time-dependent fluids. Pure viscous fluids are divided into Newtonian fluids and non-Newtonian fluids. The viscosity of the former is independent of shear stress, and the viscosity of the latter is a function of shear stress. There are plastic, swelling, and pseudoplastic fluids. The rheology of ceramic slurry usually behaves as non-Newtonian fluid.

Figure 2.12 shows the rheological curve of alumina slurry with different solid content. Fig 2.13 shows that the alumina slurry is an expanding fluid. Figure 2.14 indicates the relationship between the viscosity of 40% alumina slurry at different pH values and the shear rate. It can be seen from the figure that the rheological properties of the slurry are related to its pH value. When the pH value is less than 10 and the alumina at low shear rate The viscosity of the slurry decreases with the ascent of the shear rate, and the viscosity of the alumina slurry increases with the rising of the shear rate when the PH value is greater than 10 and at a high shear rate. When the PH value is 11, the viscosity value reaches the minimum. Therefore, in order to make the slurry in the best stable state, the PH value should be controlled within the range of 11-12.7. (Vallar, 1999)

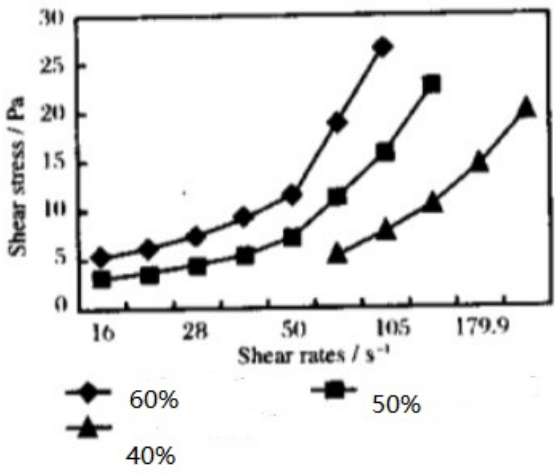

Figure 2.12: The rheological curves of Alumina slurry with different contents

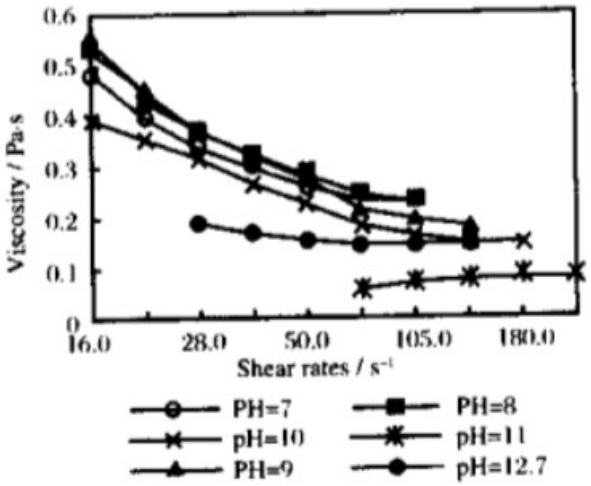

Figure 2.13: The relationship between the viscosity of Alumina slurry and shear rate

In the experiment, 18 mL of paraffin wax and 2 mL of hot melt adhesive are used as the binder system, the amount of Solsperse 170,000 is 0.7 wt%, for preparing Alumina slurry which has the solid phase content is 47 vol%, 50 vol%, 53vol%, 56 vol% , respectively. Viscosity tests were performed on slurries with different solid phase amounts at 85°C by HAAK Rheostress 6000 rheometer. Figure 2.14 shows the change curve of Alumina slurry viscosity with solid phase content when the shear rate reaches 100 s-1. The viscosity of Alumina slurry gradually rises with the ascent of solid phase content (47 vol%~56 vol%). When the solid phase content reaches 56 vol%, the viscosity of Alumina slurry reaches 8.30 Pa· s. The reason is that as the amount of solid phase increases, there are more and more Alumina particles in the slurry, and the distance between the particles becomes shorter and shorter due to compression, so there are more opportunities for Alumina particles to contact each other. Therefore, the resistance of the slurry in the flow process will also increase with the rising of the amount of solid phase. And the viscosity of Alumina slurry will increase with the addition of solid phase. (Wang J, 2007)

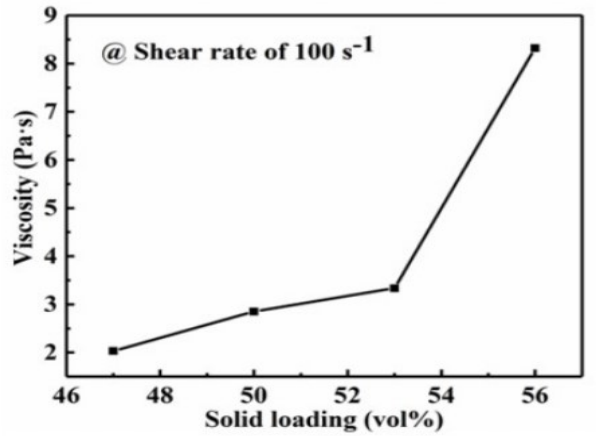

Figure 2.14:The curve about change of alumina slurry viscosity with solid content

2.8 The Review to the Process Ceramic Sintering

Ceramic sintering is the process that the ceramic green body is densified at high temperature. As the temperature rises, there are some powder particles with a larger specific surface and higher surface energy in the the ceramic green body, which try to change in the direction of reducing the surface energy, and continue to migrate substances. Then the grain boundaries move with it, and the pores are gradually eliminated, resulting in shrinkage, which makes the green body becomes a dense porcelain with a certain strength. The driving force for sintering is surface energy. Sintering can be divided into two types which are liquid-phase sintering and pure solid-phase sintering. The sintering process is of great significance to ceramic production. In order to lower the sintering temperature and expand the firing range, some additives are usually added as fluxes to form a small amount of liquid phase to promote sintering. For example, adding a small amount of silicon dioxide can promote the sintering of barium titanate ceramics, and adding a small amount of magnesium oxide, calcium oxide, and silicon dioxide is able to promote the sintering of alumina ceramics.

The research of testing the density of alumina ceramic by Archimedes' Method shows that compared with the alumina green body that has not undergone any heat treatment, the shape of alumina grain is irregular, the grain size is obviously grown, and the alumina is arranged tightly without the existence of pores, which indicates that the alumina body basically becomes dense after sintering at 1600℃. By using the Archimedes' method to test the density of the sintered alumina ceramics, the test result is 3.92 g/cm3, which is close to the theoretical density of alumina ceramics (3.98 g/cm3). It further shows that the alumina ceramics sintered at 1600℃reach a higher density. (Li Jiang et al, 2001) Figure 2.15 suggests that Shrinkage values of the alumina ceramic sintered with different holding times. It can be concluded that the shrinkage in Z direction is quite different from that in X or Y directions. The shrinkage in Z direction ranges from 3.2% to 4.8%, the shrinkage in X direction is ranging from 1.6% to 2.6%, and the shrinkage in Y direction has a range from 1.2% to 2.5%. The shrinkage in Z direction is equal to 1.8 times as much in X direction or Y direction. What's more, the shrinkage rises as the holding time ascends during sintering process. (Yu Pan et al, 2020)

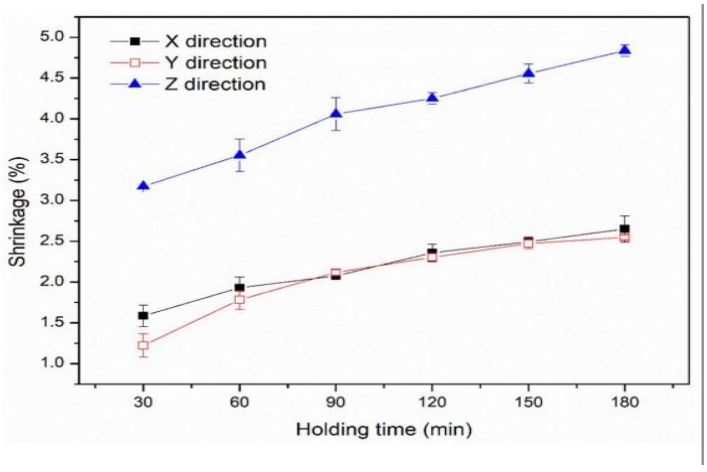

Figure 2.15: Shrinkage of alumina ceramic sintered with different holding times.

J. H PENG used alumina with a particle size of 4-8nm and 50-100nm as raw materials, and used Ar-O2 mixed gas as plasma gas for microwave plasma sintering. His experiment showed that the alumina green body with a grain size of 4-8nm could be completely dense after sintering for 15 minutes. While the alumina green body with a grain size of 50-100nm sintered under the same conditions had the relative density which could only reach 89% of the theoretical density. (Li Jiang et al, 2001) In the research of using high-purity alumina with particle sizes of 0.2 μm and 1.8 μm as raw materials, and magnesia and silicon oxide as additives for atmospheric sintering at a sintering temperature of 1460°C. The research indicated that the alumina body with a particle size of 0.2μm was almost completely dense (relative density greater than 98%) after 100 minutes, while the body with a particle size of 1.8μm was far from dense (relative density is less than 85%), which also showed that the finer the alumina particles, the easier it was to sinter and the lower the sintering temperature was. (Akira Nakajima et al, 1996)

CHAPTER 3

RESEARCH METHODOLOGY

3.1 Introduction

In this project, the main focus is a novel approach to design a compact single screw extruder to be used on FDM printer. In order to achieve this objective, Computer-Aided Design (CAD) software is used for drafting out the 3D model of the compact single screw extruder. Here, the software SOLIDWORKS is introduced to design the model of three-dimensional screw extruder. The process includes the design of important parts, such as motor, extruder screw, hopper, barrel and heating block.

3.2 The Design of Motor

In order to drive the screw extruder, the gearbox stepped motor is chose instead of normal stepped motor.

In the motor casing, the bottom plate of gearbox separates the motor casing

into the motor main body part and gearbox part composed of the stator and rotor. The variable gear set is arranged in the gear box, and a gear hole is provided in the middle of bottom plate of the gearbox. The rotor shaft gear of the rotor passes through a gear hole and extends into the gearbox to mesh with the first gear of the change gear set. The bracket of first gear is arranged in the gearbox consisted of the cover plate and the bottom plate, there is an output shaft fixed at the coaxial location of the first gear bracket and the rotor shaft. The second gear hole is provided at the middle location of the first gear bracket. The pinion of the gear set extends from the second gear hole and meshes with the gear on the output shaft; the other end of the output shaft is fastened by the cover plate. The part of the output shaft extending out of the cover constitutes the output shaft of the gearbox stepped motor. (Liptak and Bela G, 2005)

Figure 3.1: Gearbox stepped motor

Compared with common stepped motors, gearbox stepped motors have the advantages shown below:

(1) The angle of motor rotation is proportional to the number of pulses;

(2) The motor still has the torque when it stops

(3) Since the accuracy of each step is 3-5%, and the error of one step will not be

accumulated to the following up steps, it has excellent location accuracy and movement repeatability;

(4) Stable start-stop and reverse response;

(5) Since there is without brush, the gearbox stepper motor has higher reliability and the service life of the motor depends only on the one of the bearing;

(6) The response of the motor only depends on the digital input pulse, so open-loop control can be accepted, which makes the composition of the gearbox stepper motor relatively simple and cost-controlling

(7) Since the speed is proportional to the pulse frequency, so there is a relatively wide speed range. (Shan Zhengqiang et al, 2000)

Finally, a proper gearbox stepped motor has been chose to drive the screw shown in table 3.1 with its torque/speed curve performing in red line shown in the figure 3.2.

Table 3.1: The specifications of gearbox stepped motor

Phase	2 Phase
Step Angle	0.36 °/Step
Current	2.0 A/Phase
Resistance	1.73±10% Ω/Phase
Inductance	3.2±20% mH/Phase
Holding Torque	1.5 N*m
Ratio	1:5

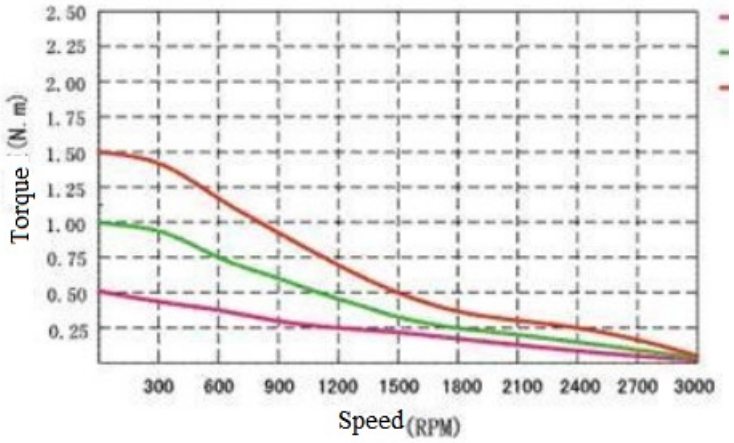

Figure 3.2 Torque/speed curve

The motor speed usually increases with the decline of its torque. In order to drive the screw for extrusion, it is necessary to keep the speed ranging from 50RPM to 100RMP. The reason is that if the screw speed is too high, the plasticizing time will be shortened correspondingly, the pressure on the material will increase, but the mixing will become worse, and the shear friction heat between the barrel and the screw will increase and the thermosetting plastic is heated unevenly. Therefore, the rotation in the project will be set as 100RMP and combined with the figure 3.2, the screw will have the maximum torque, relatively.

3.3 The Design of Extruder Screw

As the heart of the extruder, the screw has a very important influence on the quality and output of the extruder. The extrusion process indicates that the screw works at high temperature with certain corrosion and strong wear. So, the screw need to meet the requirements as follow:

(1) high temperature resistance and no transfiguration under high temperature

(2) excellent wear resistance with long service life

(3) corrosion resistance

(4) good cutting performance

The main function of a screw is the material conveying, heat transfer plasticized materials, material mixing and metering. For the project here, the aim is to design a compact screw extruder for desktop 3D printer. So the screw will be a small scale, it can not be too large. By looking for the store online in Taobao and combine with the literature reviews, the length of the screw for ceramic printing is between 80-90mm, roughly. (Ben Yue et al, 2016) So one kind of screw widely sold for ceramic printing has been introduced to the project, which has the length of 82mm. The model is shown below in Figure 3.3.

Figure 3.3: The model of the screw

The next step is to design the model by the CAD and the part of parameters are shown in Figure 3.4.

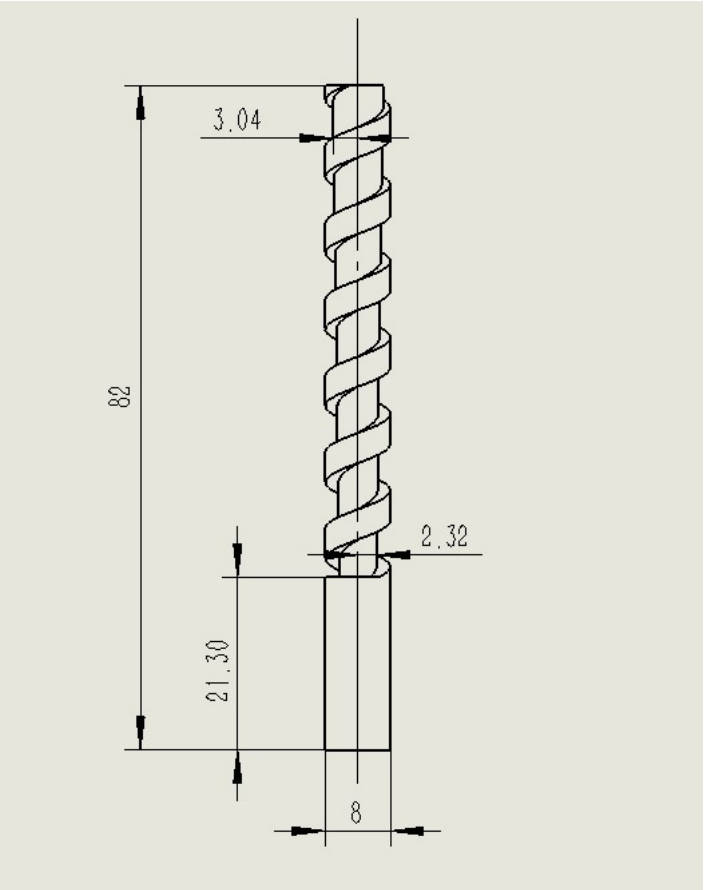

Figure 3.4: Parameters of the screw

The Screw channel depth is one of the most important components in screw design. The channel depth usually gradually reduces along the transition (or compression) section which permits more work to be exerted on the material. The ratio of the feed zone channel depth to the meter zone channel depth which is called "compression ratio", should be generally controlled at the range from 1.5:1 to 4.5:1. But here, the change of channel depth between the feeding section and metering section is very small. By the calculation, the compression ratio is equal to about 1.61, which is still within the scope required.

And the L/D ratio is the ratio of the flighted length of the screw to its outside diameter. The investigation in the market shows that there are two kinds of screws which are sold well. One has the flighted length of 56mm with diameter 8mm, and

another one has the flighted length of 80mm with diameter 10mm. It can be concluded that the range of L/D ratio is between 7:1 and 8:1. Therefore, in order to control the L/D ratio in that range, the flighted length is set at 60.7mm and the diameter is 8mm. So the L/D is equal to 7.59:1.

The helix angle is the angle of the screw thread relative to a plane perpendicular to the screw plane. If the helix angle is too large, the plasticizing time cannot be guaranteed and the plasticizing quality of the screw will be reduced. If the helix angle is too small, the volume of the channel will decrease, which will affect the extrusion volume. The standard helix angle is calculated as follows:

$$Helix\ Angle = \arctan\frac{Lead}{\pi D} \tag{3-1}$$

The equation 3-1 shows that the size of helix angle is proportional to the pitch and inversely proportional to the diameter of the screw. The helix angle must be controlled at the range from 15° and 45°. The length of pitch (P) is usually ranging from 1.25 to 2 times diameter of screw (D). Therefore, referring to the two screws for ceramic printing mentioned above, they have the same pitch which is 10mm by the measurement. Then combined with the diameter determined which is set at 8mm, from the figure 3.5. It meets the equation P=1.25D. Therefore, the helix angle in the extruder screw designed will be calculated by the equation above (Noted that the lead is equal to twice the pitch here):

$$Helix\ Angle = \arctan\frac{10\times 2}{8\pi} = 38.5° \tag{3-2}$$

So the screw designed has a helix angle of 38.5° which meets the requirement.

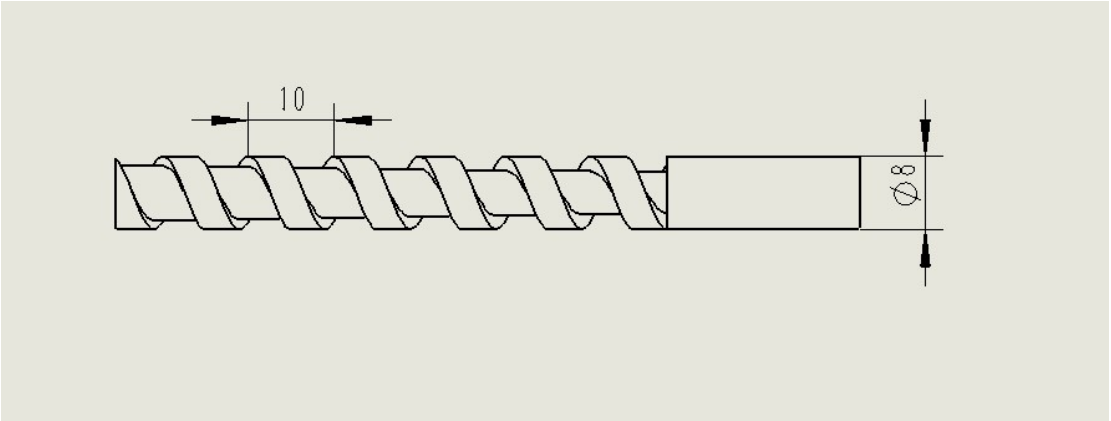

Figure 3.5: The pitch and diameter of the screw

3.4 The Design of Hopper

The feeding system is very important because an efficient feeding system is needed to ensure consistent extrusion. In order to ensure consistent feeding, the material hopper is designed to have a certain angle of repose. Studies have shown that the angle of repose is an important parameter during designing the hopper, and it is the steepest descent or inclination angle that can be tilted relative to the horizontal plane without collapsing. At this angle, the material on the inclined surface is at the edge of the sliding. The angle of repose usually changes from 0° to 90°. The shape of the material influences the angle of repose. Smooth, round sand cannot be stacked as steeply as rough, interlocking sand. The angle of repose may also be influenced by adding solvent. (Mehta, A, 1994) When the materials are round and smooth, they will have a smaller angle of repose. For sticky and fine materials, they generally have a high angle of repose. The alumina-LDPE composite is in the form of coarse powder and has a slight stickiness to it. Therefore, the alumina-LDPE composite material will have a higher angle of repose. (Teferra, 2019) The design of the hopper should have the angle of repose of Alumina-LDPE to ensure that it is always fed into the inlet. The research shows that the range of the angle of repose for granulated

ceramic powders with nice flow is usually from 30° to 40°. (K.G. Ewsuk, 2001)

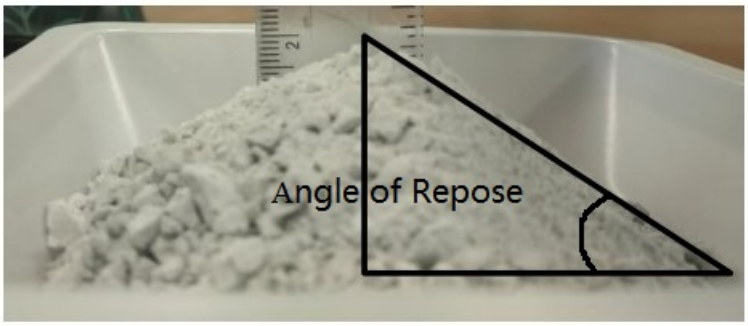

Figure 3.6: Angle of Repose

Hence, the hopper designed is shown in figure 3.7 where the insert creates an angle of about 30˚ by the calculation. This helps to funnel material into the extruder screw which will feed the material to the nozzle.

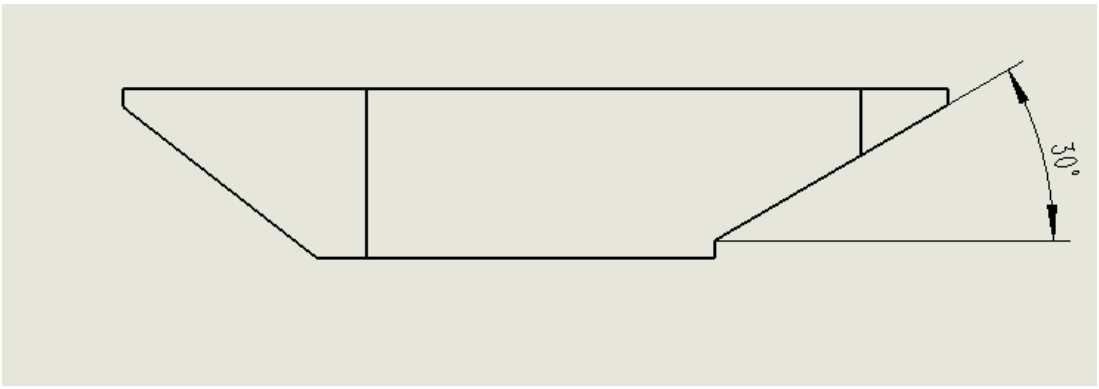

Figure 3.7: The determination of angle of repose in the hopper design

The position of hopper is one of influencing factors to the effect of screw extrusion, When the distance H1 between the entrance of hopper and the top of the screw is too large, the screw has a poor retreat effect on the ceramic, which can not accurately control the extrusion and stop of the ceramic. And there will be ceramic overflow at the nozzle in the non-printing state. If the distance H1 between the entrance and the top of the screw is too small, the pushing effect of the screw will be

greatly weakened. Generally, the ratio of distance H1 between the entrance of hopper and the top of the screw to the length of screw H is equal to about 0.4, which has a better extrsion performance, which is shown in Figure 3.8. (Cong Riyuan, 2019)

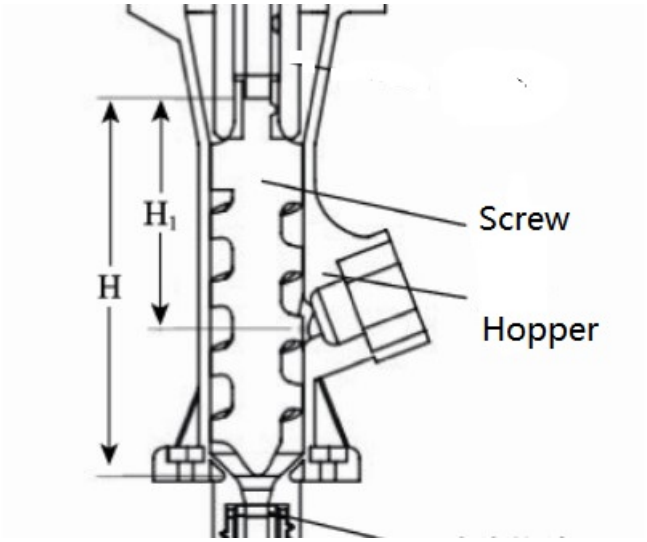

Figure 3.8: The position of hopper relative to the screw

The material of hopper is usually plastic because it has less weight. And in this project, the hopper is pre-made by 3D printer and the model is shown as follows. For the selection of materials, PETG is usually chose to manufacture the hopper because it has good toughness, impact and chemical resistance. Therefore, it ensures that the hopper will not chemically react with the materials going into the hopper. In order to verify the performance of hopper made from PETG, there will be simulation in the follow-up analysis.

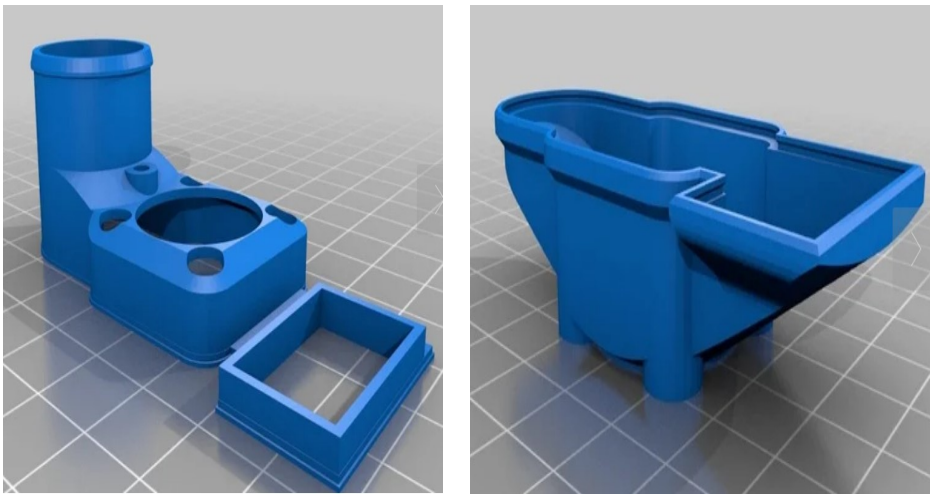

Figure 3.9: The model of hopper

3.5 The Design of Barrel

Because the pressures generated within an extruder can reach very high values, the barrel is constructed to withstand these high pressures without distortion. The barrel, therefore, is made from alloy tubing or pipe which has good wear and corrosion resistances, and barrel is usually equipped with the heat sink absorbing the heat during the extrusion processes. Usually, the barrel and heat sink with the nozzle are integrated showed in figure 3.10.

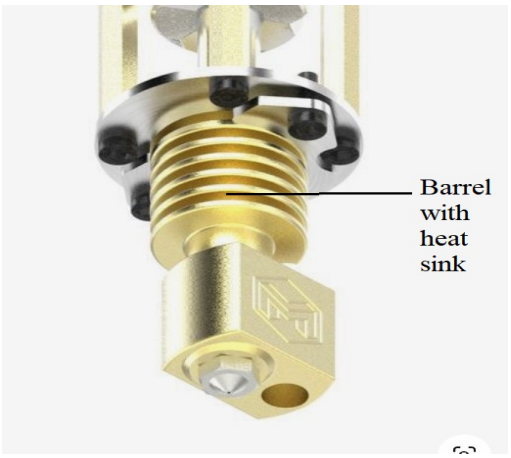

Figure 3.10: Barrel integrated with heat sink

The gap between the screw and the barrel has a very important impact on the performance of extruder. The gap here refers to the unilateral clearance between the inner wall of the barrel and the outer wall of the screw. The size of the gap determines the flow rate, return flow rate, and shear stress of the extruder. As the gap increases, the amount of extrusion will decrease. When the gap reduces, the shearing force of the extruded material will increase, and the friction between the screw and the barrel will be too violent, resulting in locking. By looking through the literature, it is concluded that the gap should be controlled at about 0.25mm between the barrel and screw. (Cong Riyuan, 2019)

3.6 The Design of Nozzle

The nozzle is the part which is responsible for the flow of material at the desired size. Its design should aid in the process of achieving constant flow velocity at the outlet and there should be enough pressure buildup in the nozzle region to have continuous extrusion. (Dylan T.J. Drotman et al, 2015) Usually nozzle size ranges from 0.1mm to 1mm and 0.4mm is considered the standard nozzle size of a 3D printer. So the diameter of nozzle in the project will be set at 0.4mm.

Line width is a key parameter during printing. And the minimum line width can be thought about when the flat width and the nozzle size has the same value, which makes sure that the oblong shape is consistent and formed. The relationship among diameter, layer height and line width is showed as follows:

$$\text{Line Width} = \text{Nozzle Size} + \text{Layer Height} \quad (3\text{-}3)$$

Usually, the layer height is about 0.2mm. So the line width in the project can be easily calculated, which is equal to 0.6mm when the flat width is equal to the nozzle size.

For ceramic printing, the speed of it is usually ranging from 30mm/s to 45mm/s. So the volumetric speed can be calculated by the formula below:

$$\text{Volumetric speed} = \text{Layer Height} \times \text{Extrusion Width} \times \text{Speed} \quad (3\text{-}4)$$

So the minimal and maximal volumetric speed will be $3.6\,mm^3/s$ and $5.4\,mm^3/s$ by the equation 3-4, respectively.

$$\begin{aligned} Minimal\ Volumetric\ Speed &= 0.2mm*(0.2mm+0.4mm)*30mm/s = 3.6mm^3/s \\ Maximal\ Volumetric\ Speed &= 0.2mm*(0.2mm+0.4mm)*45mm/s = 5.4mm^3/s \end{aligned} \quad (3\text{-}5)$$

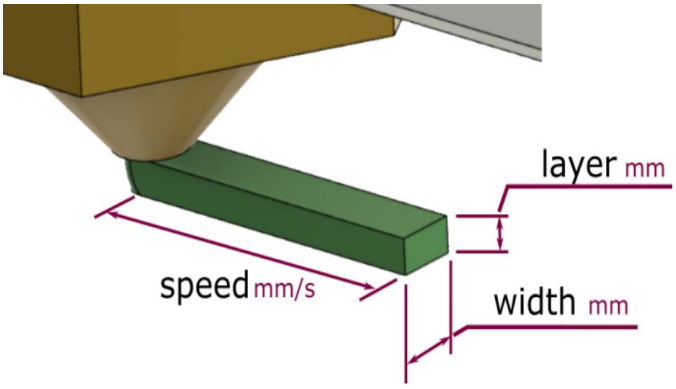

Figure 3.11: The parameters of filament

3.7 The Design of Heating Block

A heating system is required to melt the material fed into the extruder for extrusion.

The working temperature of the heating block has a range from 105°C to 135°C to melt the Alumina-LDPE composite material. Figure 3.12 suggests the CAD drawing of the heating block. The heating block is designed to be installed on the barrel of the extruder to ensure even heating around. The design of the beating block is that the thermal box and thermistor on the traditional filament print head can be reused on the single screw extruder. There are 2 through holes passing through the module in the longitudinal direction. The one on the left is designed to fit the extruder barrel by threaded connection, while the another is designed to fit the heating cylinder.

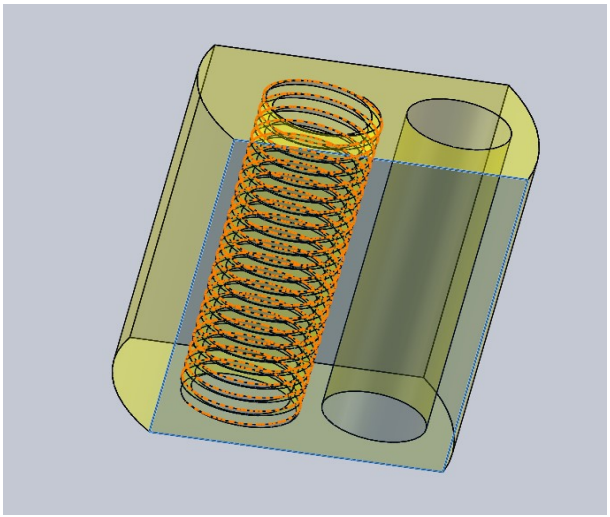

Figure 3.12: The design of heating block

When a temperature is set in the printer, the ceramic heater cartridge will be powered up and starts heating. Thermistor will feed back temperature of the heating block to the system to regulate the power send to the ceramic heater cartridge. To get accurate reading of the temperature on the barrel of the extruder, thermistor is mounted on the wall nearest to the barrel of the extruder. This helps to monitor the temperature and prevent the heating block from overheating Alumina-LDPE composite. Alumina-LDPE composite is prone to degradation when heated at temperature above 115˚C for extended period of time.

3.8 The Calculation Involved in the Design

3.8.1 Output Flow Rate Model

Making an consumption that the viscosity of the material is constant along the barrel with the constant screw speed, output flow can be easily modeled in m^3/s for the isothermal case by modeling the flow based on channel geometry.

$$Q = P * \frac{Fbd^3}{12\eta L_d} \tag{3-6}$$

The flow coefficient is usually calculated by the use of channel geometry. So operating pressure expressed in Pa for the output can be got by the equation 3-7.

$$P = \frac{2\pi\eta D^2 NH\sin(\phi)\cos(\phi)}{\frac{1}{3Ld}(\frac{Fbd^3}{\pi} + DH^3\sin^2(\phi))} \tag{3-7}$$

Then the output flow rate can be determined by the equation 3-5. (Dylan T.J. Drotman, 2015) The extrusion variable definitions and flow coefficient are shown in Table 3.2 and Figure 3.12, respectively.

$$Q = 0.5\pi^2 D^2 NH\sin(\phi)\cos(\phi) - \frac{\pi DH^3\sin^2\phi P}{12\eta L} \tag{3-8}$$

Table 3.2: Extrusion variable definitions

Q	Output flow rate (m^3 / s)
P	Output pressure (Pa)
F	Flow coefficient
L_d	Length of barrel (m)
b	Channel width (m)
d	Channel height (m)
η	$m(℃) * \gamma^{n-1}$
m	Consistency index function of Temperature (T)
n	Power law
γ	Viscosity (Pa.s)
D	Inside diameter of barrel (m)
N	Screw revolution (rpm)
H	Channel depth of the screw (m)

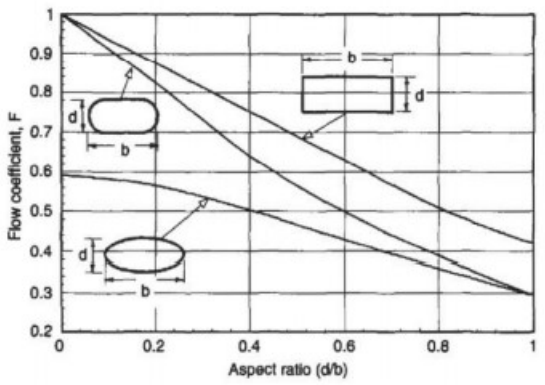

Figure 3.13: Flow coefficient for a given channel geometry

By measuring the parameters of the screw shown in Figure 3.13, the flow rate can be easily calculated.

Table 3.3: Critical parameters of the screw

L	Length of barrel	95.41 mm
N	Screw revolution	1.67 rps
P	Pressure	
D	Inside diameter of the barrel	8 mm
H	Channel depth height	1.4 mm
ϕ	Helix angle	38.5°
η	Viscosity	10000cps

The final result is shown as follows:

$$Q = 0.5\times\pi^2\times(8\times10^{-3})^2\times1.67\times(1.4\times10^{-3})\times\sin38.5°\times\cos38.5° - \frac{\pi\times(8\times10^{-3})\times(1.4\times10^{-3})^3\sin^2 38.5°\times P}{12\times10\times(95.41\times10^{-3})}$$
$$Q = 3.60\times10^{-7} - 2.33^{-12}P \quad (3\text{-}9)$$

3.8.2 Max Output Pressure

When the pressure drop at the exit of the extruder is high, Output flow rate Q will be 0, which means that the drag flow and pressure flow have the same value. This is where the material stops squeezing out due to the buildup of too much pressure. This pressure is so useful that it can determine the point when the extruder stops extruding. (Dylan T.J. Drotman, 2015) The max output pressure can be calculated by the equation as follows:

$$P_{\max} = \frac{6\pi DLN\eta}{H^2 \tan(\phi)} = \frac{6\pi \times (8\times10^{-3}) \times (95.41\times10^{-3}) \times 1.67\times10}{(1.4\times10^{-3})^2 \times \tan 38.5°} \quad (3\text{-}10)$$
$$= 154113.33\,pa$$

Then move the value of $P_{\max}$ in equation 3-7 to the equation 3-6:

$$\begin{aligned} Q &= 3.60\times10^{-7} - 5.03\times10^{-14} P_{\max} \\ &= 3.60\times10^{-7} - 2.33^{-12} \times 154113.33 \\ &= 0 \end{aligned} \quad (3\text{-}11)$$

It can be concluded that when the output pressure reach the maximum value, the output flow rate Q will be 0. What's more, the pressure drop at the exit of the extruder will be usually smaller than max output pressure.

3.9 The Assembly of Screw Extruder

After the design of the parts above, the final process is to connect and integrate all of them. Figure 3.14 below shows the model of the whole screw extruder by SOLIDWORKS. And this small section will cover how to assembly this screw extruder.

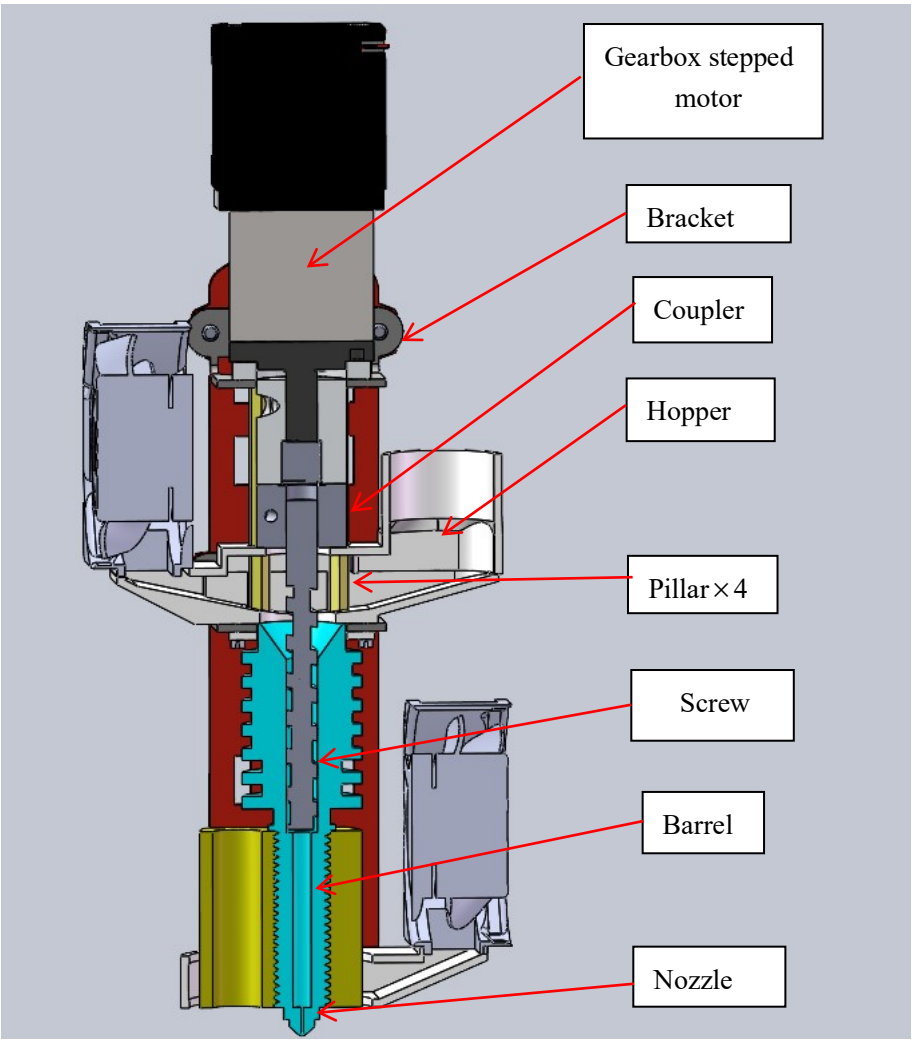

Figure 3.14: The cross section of screw extruder designed

The detailed process is shown as follows:

(1) First fit the bracket over the motor by the screw connection.

(2) Then connect the coupler with rotor part of the motor, and also the screw at another end.

(3) In order to fix the hopper on the extruder, it is necessary to use four pillars shown in the Figure 3.14, which connect with the bracket and the hopper (There will be four small holes and one big hole in the center for the four pillars and the screw to penetrate, respectively, shown in the Figure 3.15). At the bottom of the hopper, there will be another bracket to support it, which also fits the four pillars.

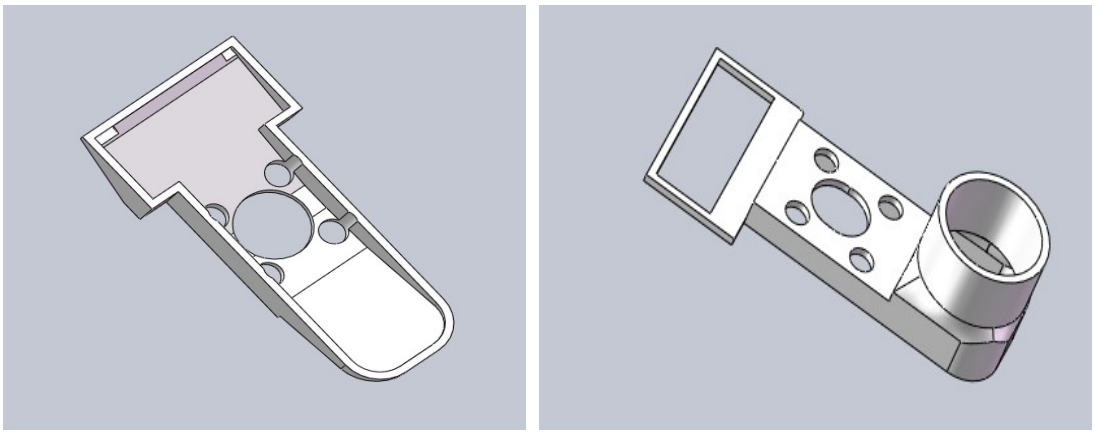

Figure 3.15: The model of hopper designed

(4) The next step is to assemble and fit the barrel. Here, the barrel is designed to equipped with a steel gasket shown in Figure 3.14, and it relies on the gasket to be connected with the bracket which is the one at the bottom of the hopper by the screw connection.

(5) And then, fix the heating block on the barrel. There will be the thread on the barrel, which has the effect of fitting the heating block to the barrel.

(6) At last, assemble the fans and the plates, shown in Figure 3.16. The fans here play the role of heat dissipating. And for the plates, they enhance the fixing of the whole screw extruder.

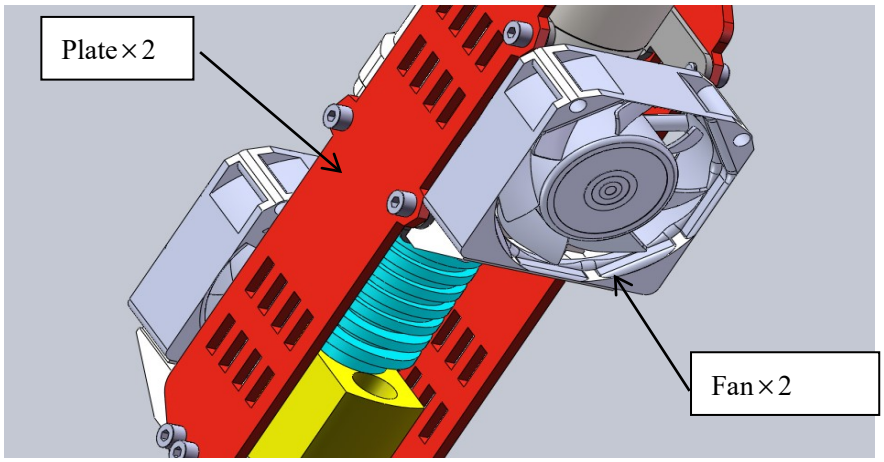

Figure 3.16: The assembly of the fans and plates

3.10 The Simulation to the Screw Extruder

To prove the capability of the compact screw extruder, a battery of tests will be done including simulations and actual testing. Computer Aided Engineering (CAE) simulations are done to validate the performance of the compact single screw extruder. Flow Simulation is a powerful tool to understand and optimise the design of the single screw extruder. With the prototype of the compact single screw extruder, testing will be done to verify its performance. And the detailed process will be covered in this part.

First of all, because of the Flow Simulation is a plug-in component in Solidworks, the first step is to open the 3D model of screw extruder designed and simplify it, shown in Figure 3.17 and Figure 3.18.

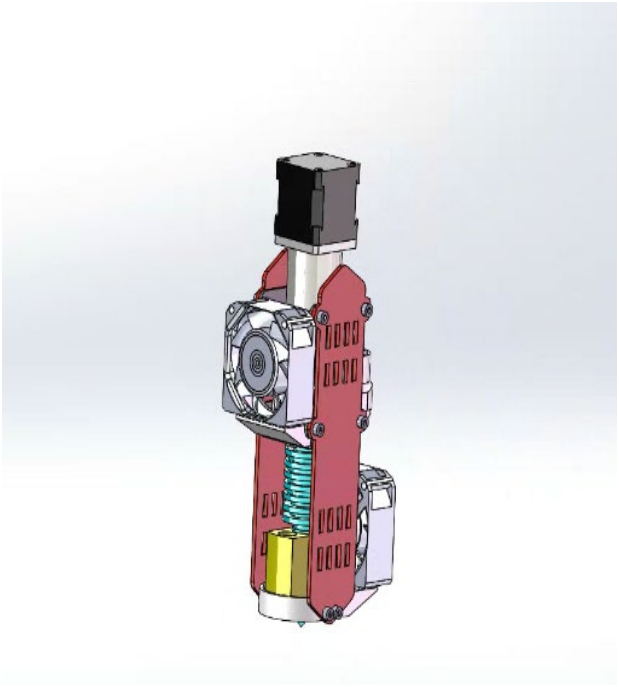

Figure 3.17: The model of screw extruder designed

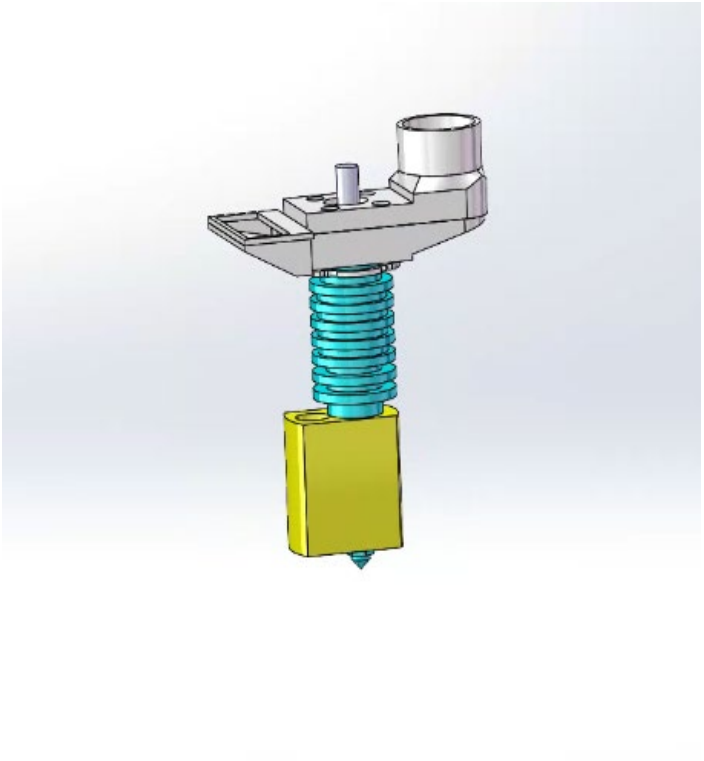

Figure 3.18: The model after being simplified

Then click on the function Guide in order to set up the analysis process which includes the setting of Analysis Type, and Initial and Environmental Condition. The process is to check the option of heat conduction in solids, check gravity, and modify the direction according to the actual gravity direction of the model. Then, the pressure is set to 101325Pa, the temperature is set to 20.05 degrees Celsius, and the flow rate of each component is set to 0, which means that the simulation is carried out at room temperature and pressure, shown in Figure 3.19.

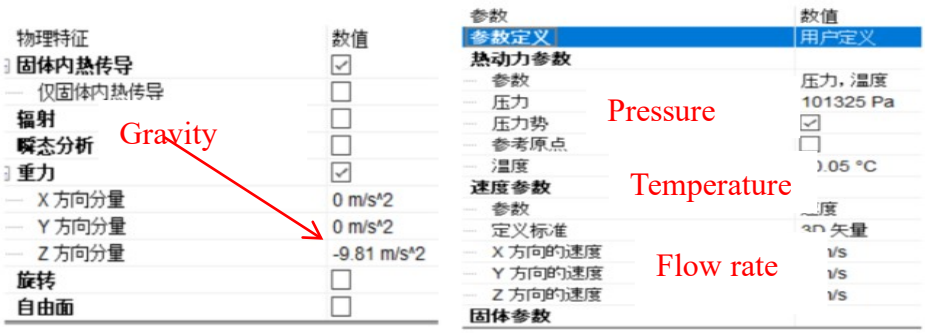

Figure 3.19: The setting of Analysis Type, and Initial and Environmental Condition

After that, the step is to set the boundary conditions including material of components of the extruder designed, temperature of heat source and rotation of screw, shown in Figure 3.20.

For the temperature of heat source, in order to identify the ideal temperature of extrusion for Alumina-LDPE composite, the heating block was heated to different temperature. Table 3.4 summarizes the result of extrusion at different temperature. (Dow Chemical, 2011) It shows that when the temperature is set at 125℃, it will have the most proper effect for extruding. So the temperature of heat source is set as 125℃, showing in Figure 4.28.

Table 3.4: Summary of the results when extruding at different temperature

Temperature (˚C)	Result
100 to 120	Temperature too low to melt Alumina-LDPE composite.
125	Ideal temperature to extrude Alumina-LDPE composite.
130 to 135	Temperature too high which causes Alumina-LDPE composite to degrade in short time.

And then, the process is setting the analysis grid. Since Flow Simulation will automatically determine the fluid and solid, what to do is only to adjust the grid size. Here, the global grid size level is adjusted to 3, corresponding to the basic grid. Due to the small size of the nozzle, to make sure of the calculation accuracy of position, it is necessary to further perform local grid control on this area, and adjust the fluid grid, solid grid and handover grid level at the nozzle to 7, shown in Figure 3.20.

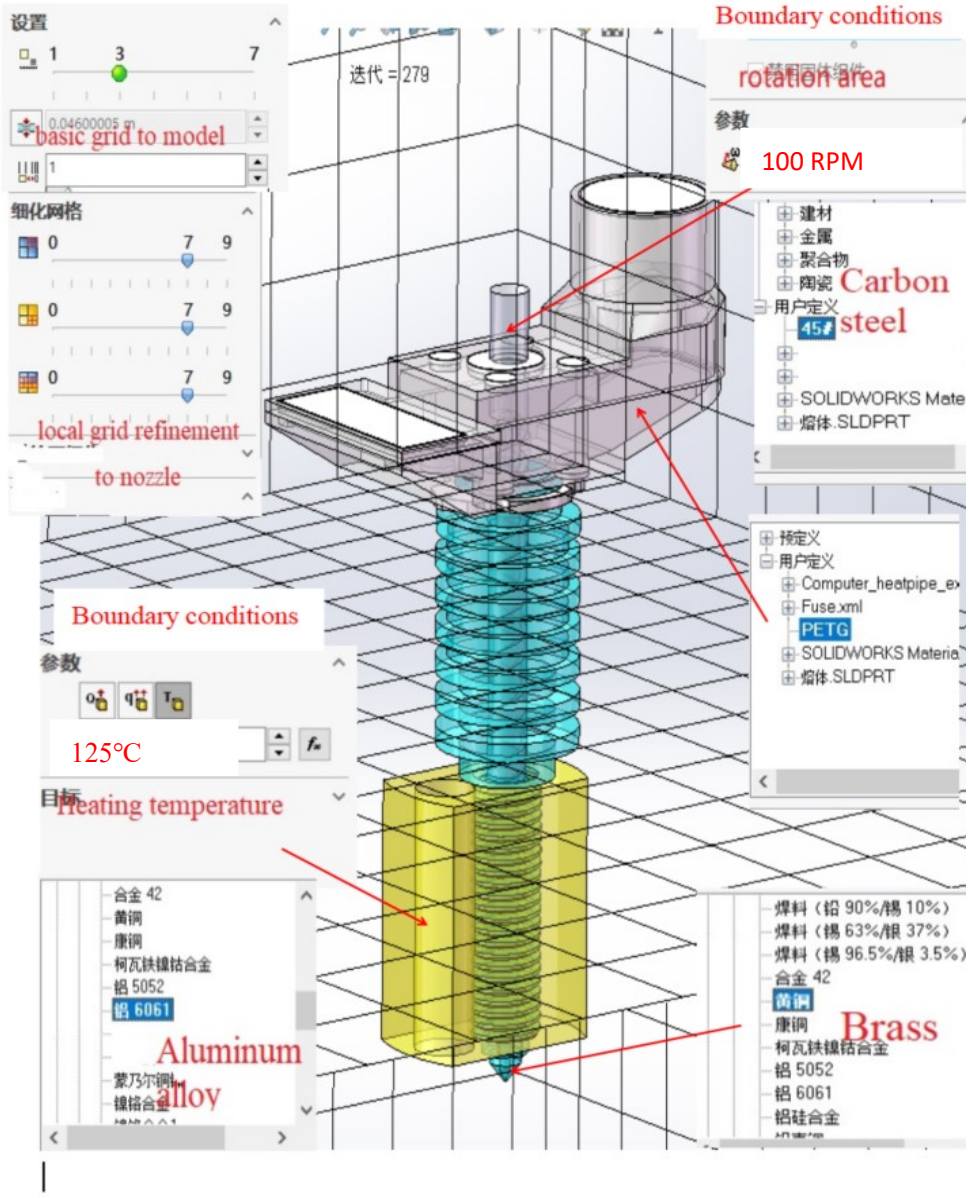

Figure 3.20: The setting of boundary conditions and analysis grid

Finally, after all parameters and data being set up, the last process is to run the simulation program. And the results and discussions to the simulation done will be involved in Chapter 4.

CHAPTER 4

RESULTS AND DISCUSSIONS

4.1 Introduction

In this section, it will cover the outcomes of the simulation part in chapter 3, and at the same time, it will also involve in comparison between the data by calculation and by simulation. And the aim is to test the performance of screw extruder designed in the project.

4.2 The Static Pressure of Screw Surface and Ceramic Slurry

The static pressure diagram can obtain the result of the static pressure of the fluid in the analysis, and the pressure of the fluid acting on the solid surface can be obtained through the static pressure value, which can be used to make a preliminary assessment of the strength of the structure.

From the figure 4.1, the pressure is greater at the inlet, and gradually decreases toward the head of screw. From the knowledge of fluids, the pressure is

small where the flow rate is high. Therefore, it is judged that the velocity of alumina-LDPE particles is the smallest at the inlet. After being extruded by the screw, it gradually becomes a slurry, and its flow rate gradually increases.

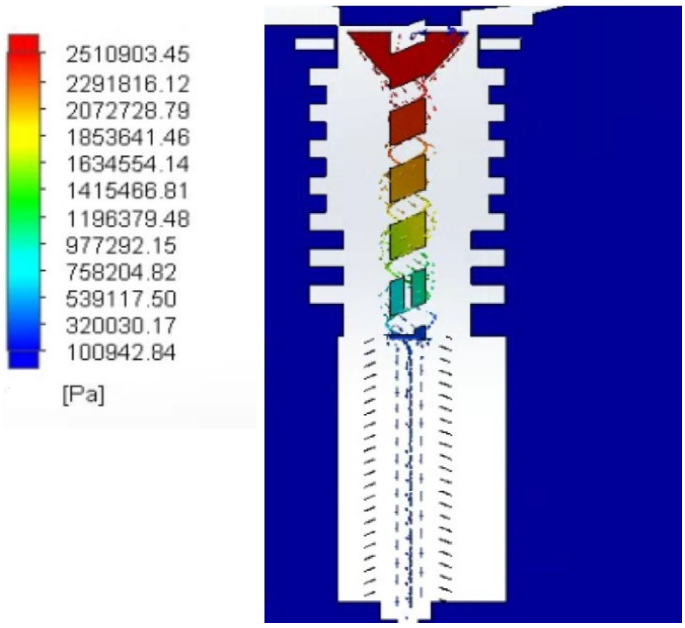

Figure 4.1: The pressure on ceramic slurry during extrusion

As shown in figure 4.2, since the screw is in close contact with the slurry fluid in the barrel, its overall surface pressure distribution is roughly the same as the fluid area. Above the screw, the slurry enters at a lower speed from the external inlet, and the pressure is greater. After the slurry enters the barrel, it is accelerated by the rotation of the screw, the speed increases slightly, and the pressure gradually decreases. The reason is that the speed is small where the pressure is large, relatively.

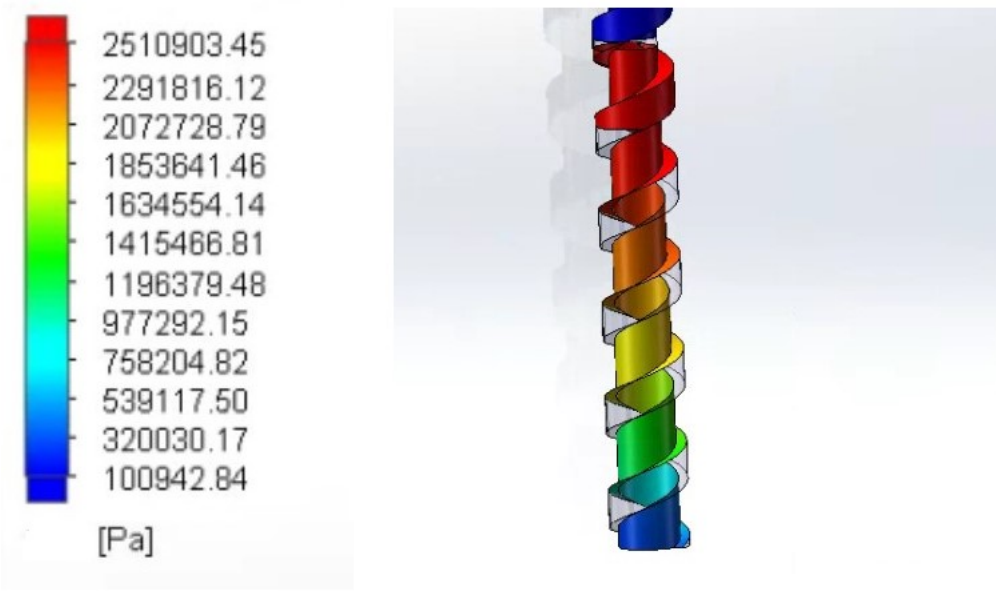

Figure 4.2: The pressure on the screw surface in the barrel

4.3 The Analysis of Heat Transfer

The surface temperature figure can be used to view the temperature on the surface of the model to facilitate the grasp of its temperature distribution. It is a common result of obtaining the temperature distribution of the model in the heat flow field analysis. The figure 4.3 shows the temperature distribution of screw extruder by using PETG to make the hopper.

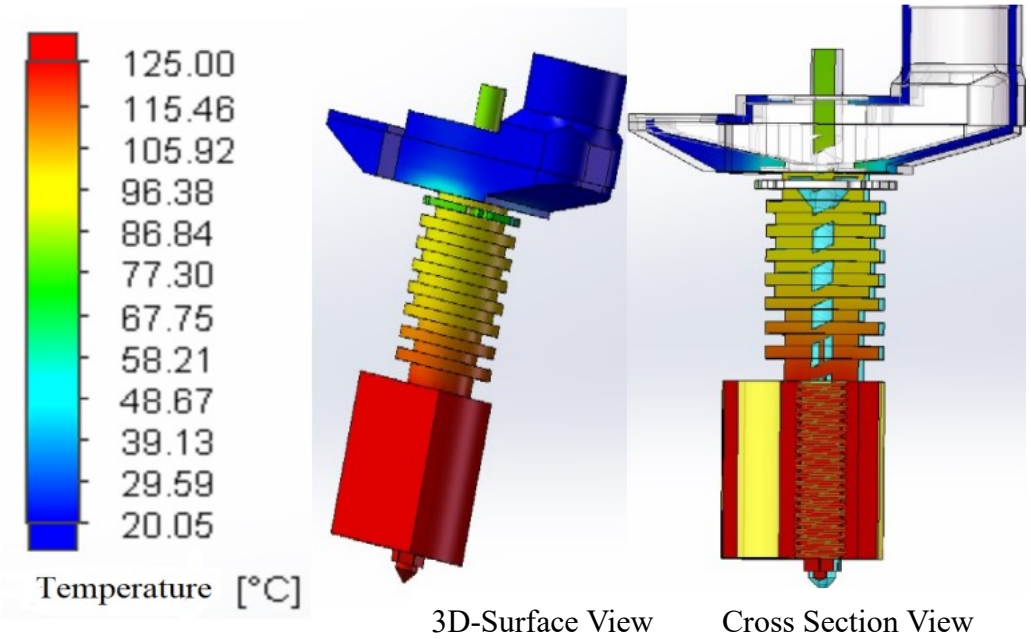

Figure 4.3: Temperature distribution of the model

It can be concluded that surface temperature of hopper at its inlet is lower than 30℃, and the temperature increases to about 50℃ at its outlet, which is lower than the heat distortion temperature of PETG (69~70℃). On the one hand, the hopper made from PETG will not deform. On the other hand, the glass transition temperature of alumina and LDPE pallets is around 80℃, so it ensures that alumina and LDPE pallets will not melt in the hopper, occurring material blocking at the outlet of hopper, which verifies that the hopper made from PETG can be used in this project for 3d printing.

4.4 The simulation to Flow Trace and Speed

The flow trajectory graph can be used to view the entire fluid flow path of the analysis. Through the flow trajectory graph, we can know whether the flow characteristics of the entire analysis meet our expected design, and it can also be

used to check whether there are setting problems in the simulation.

In order to verify whether the fluid movement process is consistent with the actual situation, the flow trajectory of the model is checked, shown in Figure 4.4. It is concluded from the flow trace graph that the fluid enters from the inlet, then flows through the internal spiral structure, and then ejects from the nozzle. In this process, the slurry can move down smoothly without cross-coincidence. The speed change during the fluid flow is consistent with the actual situation, which indicates that the simulation in this project meets the actual requirements.

Figure 4.4 also shows the speed distribution from barrel inlet to the nozzle and measuring the velocity in the nozzle is about 34mm/s which meets the requirement of speed for ceramic printing.

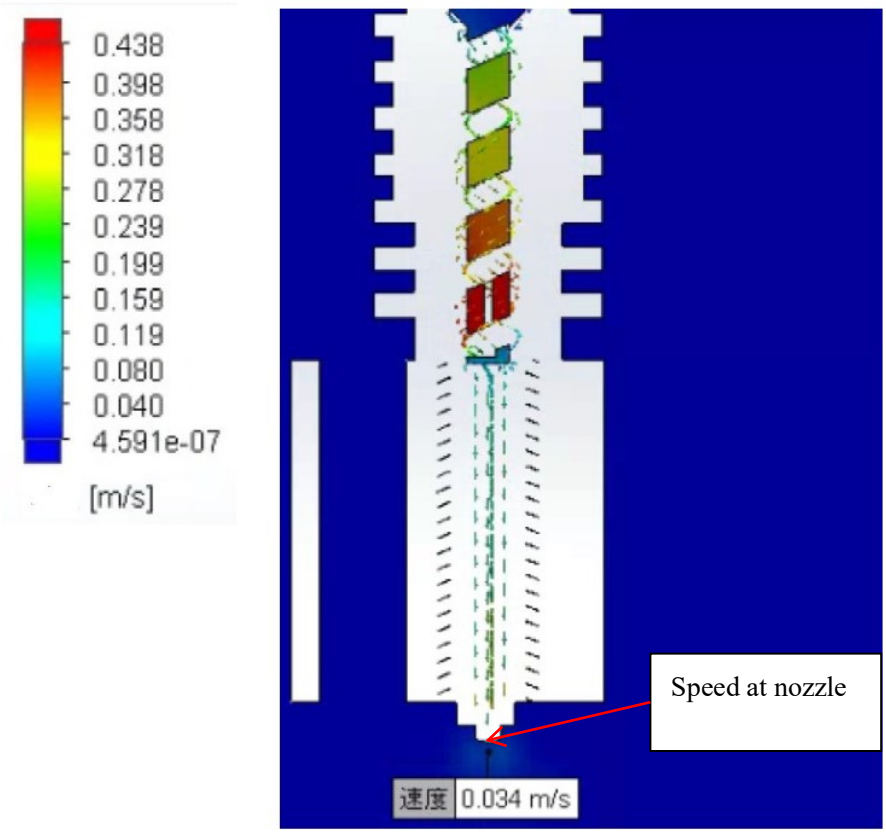

Figure 4.4: Flow trace with speed distribution

4.5 Outlet Pressure Measurement

Figure 4.5 shows the outlet pressure distribution which is ranging from 108592.14 Pa to 109425.25 Pa. By the calculation in the chapter 3, the max output pressure is 154113.33 Pa which is larger than the outlet pressure. It can be concluded that there will be output flow rate at the outlet which is consistent with the actual situation.

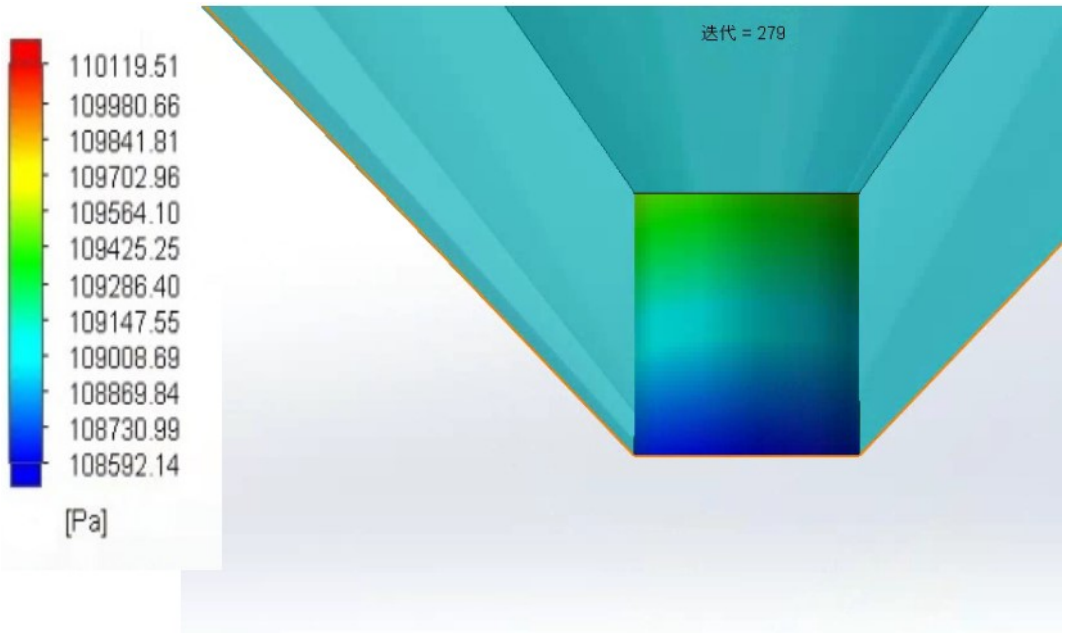

Figure 4.5: Outlet pressure measurement

CHAPTER 5

CONCLUSIONS AND RECOMMENDATIONS

5.1 Conclusion

Based on testing done on the prototype of compact single screw extruder, the objective of designing a compact single screw extruder that is capable of extruding Alumina-LDPE composite has been fulfilled. This is done by using CAD software to draft out the CAD model of the compact single screw extruder. After the drawing was finalised, the process is to simulate the performance of single screw extruder. Testing result has shown that the compact single screw extruder is capable of extruding Alumina-LDPE composite.

One the hand, the project has achieved the objective of designing the components of the screw extruder. It concluded that the gearbox stepped motor is chose to drive the screw and its rotation speed is controlled at 100rpm with its corresponding torque 1.5Nm. For the design of extruder screw, the screw designed has a length of 82mm with a compression ratio 1.61:1, helix angle 38.5° and pitch 10mm, which meets the requirements for extrusion. In the part of design of hopper, the hopper has a angle of repose 30° at the inlet, which ensures the better flow to the inlet. The ratio of distance between the entrance of hopper and the top of the screw

to the length of screw is equal to about 0.4, which has a better extrusion effect. For the design of barrel, it is adopted a one-piece structure, which integrated with heat sink and nozzle. And the gap between screw and barrel is controlled at 0.25mm which ensures nice flow rate.

On the other hand, this project also has reached the objective of simulation work. For the static pressure part, the static pressure on the alumina slurry and screw surface decrease gradually from the end to head of screw. In the part of heat transfer, the temperature distribution decreases from the heat block to the hopper. At the same time, it is concluded that PETG as the raw material for making the hopper in this project is practical. Then, the simulation to the flow trace verifies that the slurry can move down smoothly without cross-coincidence which is consistent with the actual situation. And then by the simulation, the outlet pressure at the nozzle is lower than the max output pressure, which ensures that there will be flow in the outlet. At last, by changing to the speed distribution graph, the speed at nozzle is 34mm/s, which is between 30mm/s and 45mm/s for ceramic printing.

5.2 Recommendation for Future Work

The limitation in the project is that the function heating of heat block is considered as the only external condition, and the heat dissipation function of the fan installed on the screw extruder is ignored. Because of the heat dissipation function of the fan, the fan relies on the fan blades to continuously rotate around the axis to make the air around the extruder circulate. By increasing the heat continuously through the continuous circulation of air, the internal and external temperature of each part of the extruder will reduce. In the future work, the same simulation will be carried out to perform the temperature distribution involving in two external conditions which are

the rotation of fans and the heating of heat block. So the analysis of experimental data will be more reasonable.

The feed rate of a compact single-screw extruder can be increased by having a larger barrel and hopper. By enlarging the diameter and size of the barrel and hopper, more materials can be transported, thereby increasing the flow rate of the materials. As a result, since the printer can work at a higher speed, the printing time can be reduced.

What's more, since the model of screw extruder has been finished, the further work can be the simulation to the static pressure on the slurry and screw surface, temperature distribution and speed at the outlet, etc by using other raw material for 3D printing.

REFERENCE

Jin Zhihao, 2000. Engineering Ceramic Materials. Xian, China: Xi'an Jiaotong University Press.

Guan Zhenduo, Zhang Zhongtai, and Jiao Jinsheng, 2011. Physical Properties of Inorganic Materials. Beijing, China: Tsinghua University Press.

Berman B, 2012. 3-D printing: The new industrial revolution. Business Horizons, 55(2), pp.155-162.

Chen Zhangwei, Li Ziyong, and Li, Junjie, 2019. 3D printing of ceramics: A review. Journal of the European Ceramic Society, 39(4), pp.661-687.

Liu Houcai, Mo Jianhua and Liu Haitao, 2008. A review of three dimensional printing technology and its application. Mechanical Science and Technology for aerospace Engineering, 27(9), pp.1187-1190.

Manicone, Paolo Francesco, Rossi Iommetti, et al, 2007. An overview of zirconia ceramics: Basic properties and clinical applications. Journal of Dentistry, 35(11), pp.819-826.

Liu W B, Xiong N, Wang T J, et al, 2015. Study on thermal shock resistance of silicon nitride ceramics prepared by sintering-HIP technique. Bull Chinese Ceram Soc, 34(1), pp.213.

Zhang Wenyan, 2013. Research Progress of 3D Printing Technology in Medical Domain. Journal of Chinese hospital directors, (12), pp.60-62.

Liu Wei, Wu Haidong, Wu Shanghua, 2017. Research Progress of Additive Manufacturing Technology for Ceramic Materials. Journal of Ceramic, 38(4), pp.451-459.

Wang Di, Yu Dongman and Li Xiaojing, 2011. Process analysis and application for rapid prototyping based on fused deposition modeling, Machinery Design & Manufacture, pp. 65-67.

Harold F. Giles, John R. Wagner, 2004. Extrusion:The Definitive Processing Guideand Handbook. America: William Andrew.

Li Xinjun, Lv Haibo and Zhou Jicheng, 1999. Progress in Research on the Binder and Debinding in Powder Injection Molding, Materials Review, 4(3), pp. 207-212.

G Bandyopadhyay and KW French, 1994. Effect of powder characteristics on injection molding and burnout cracking. American Ceramic Society Bulletin, 73(3), pp. 107-114.

R M German and K F Hens, 1992. Identification of the effects of key powder characteristics on powder injection molding. Powder Injection Molding Symposium, 47(10), pp. 55.

Cong Riyuan, Du Yungang, Lu Yue, et al, 2019. Design and Simulation Analysis of Ceramic 3D Printer Extruder. China Ceramic Industry, 26(4), pp.13-17.

Subramanian K, Vail N, Barlow J, et al, 1995. Selective laser sintering of alumina with polymer binders. Rapid Prototyping Journal, 1, pp.24-35.

Liu K, Sun H J, Wang J, et al, 2017. Techniques of 3D Printing Combined with Densification Processes for the Fabrication of Ceramic Parts. Advanced Ceramics, pp. 381-388.

Yang Z M, 2015. The rapid development of ceramic 3D printing. Office Information, 20(1), pp.16.

Chia H W and Wu B M, 2015. Recent advances in 3D printing of biomaterials. J Biolog Eng, 9(1), pp.1.

Rutz A L, Hyland K E, Jakus A E, et al, 2015. A multimaterial bioink method for 3D printing tunable, cell-compatible hydrogels. Adv Mater, 27(9), pp. 1607.

Isakov D V, Lei Q, Castles F, et al, 2016. 3D printed anisotropic dielectric composite with meta-material features. Mater Des, 93, pp.423-430.

Zhao Guifan and Yang Na, 2008. Manufacturing Process of Car. Beijing, China: Peking University Press.

Onagoruwa S, Bose S and Bandyopadhyay A, 2001. Fused deposition of ceramics (FDC) and composites. Proceedings of Solid Freeform Fabrication Symposium. pp. 224-231.

Carneiro O S, Silva A F, Gomes R, 2015. Fused deposition modeling with polypropylene. Materials & Design, 83, pp. 768-776.

McNulty T F, Mohammdi F, Bandyopadhyay A, et al, 1998. Development of a binder formulation for fused deposition of ceramics. Rapid Prototyping Journal, 4(4), pp. 144-150.

HUANG M J, WU H D, HUANG R J, et al, 2017. A review on ceramic additive manufacturing (3D printing). Advanced Ceramics, 38(4), pp. 248–266.

GRIFFITH M L, HALLORAN J W, 1996. Freeform fabrication of ceramics via stereolithography. Journal of the American Ceramic Society, 79(10), pp. 2601–2608.

Ma X L, 2013. Research on application of SLA technology in the 3D printing technology. Appl Mechan Mater, pp. 401-403 938-941.

Zhang K S, Yao L J, 2015. Key technologies of SLA 3D printing. Mechan Electrical Eng, pp. 401-403 938.

M. Kurimoto, H. Ozaki, Y. Suzuoki, et al, 2016. Dielectric properties and 3d printing of uv-cured acrylic composite with alumina microfiller. IEEE transactions on dielectrics and electrical insulation, 23(5), pp. 2985-2992.

M. Kurimoto, H. Ozaki, Y. Suzuoki, et al, 2016. Influence of filler diameter on UV transmission and dielectric permittivity of alumina composite used for stereolithographic 3D printing. IEEE International Conference on Dielectrics, pp. 971-974.

Yang K, Xu S, Li B, 2020. The influence mechanism of nano-alumina content in semi-solid ceramic precursor fluid on the forming performance: Via a light-cured 3D printing method. RSC Advances, 10(68), pp. 41453-41461.

SPOATH S, SEITZ H, 2014. Influence of grain size and grain-size distribution on workability of granules with 3D printing. International Journal of Advanced Manufacturing Technology, 70(1/4), pp.135–144.

Klosterman D, Chartoff R, Priore B, et al, 1996. Structural Composites via Laminated Object Manufacturing LOM. Solid Freeform Fabrication Symposium Proceedings. pp. 105-115.

YANG W L, WANG X F, JIANG H T, et al, 2006. Freeform fabrication of ceramics parts based on rapid prototyping technology. Materials Review, 20(12), pp. 92–95.

Don Klosterman, Richard Chartoff, Nora Osborne et al, 1997. “Lami□nated object manufacturing, a new process for the direct manufac□ture of monolithic ceramics and continuous fiber CMCs”, Ceramic Engineering and Science Proceedings, Proceedings of the 1997 21st Annual Conference on Composites, Advanced Ceramics, Materials, and Structures-B, Cocoa Beach, Florida, 18(114B), pp:113–120, 12–16 .

Y. Zhang, X. He, J. Han, et al, 2001. Al2O3 Ceramics Preparation by LOM (Laminated Object Manufacturing), Int J Adv Manuf Technol, 17, pp:531–534.

Ben Yue, Zhang Le, Wei Shuai, et al, 2016. Research Progress of 3D Printed Ceramic Materials. Materials Reports, 30(11), pp. 109-115.

WILKES J, HAGEDORN Y, MEINERS W, et al, 2013. Additive manufacturing of ZrO2-Al2O3 ceramic components by selective laser melting[J]. Rapid Prototyping Journal, 19(1), pp.51–57.

Exner, H., Horn, M., Streek, A., Ullmann, F., Hartwig, L., Regenfuß, P. and Ebert, R.,2008. Laser micro sintering: A new method to generate metal and ceramic parts of high resolution with sub-micrometer powder. Virtual and Physical Prototyping, 3(1), pp. 3-11.

Liu, F.-H.,2012. Synthesis of bioceramic scaffolds for bone tissue engineering by rapid prototyping technique. Journal of Sol-Gel Science and Technology, 64(3), pp. 704-710.

Tian, X., Sun, B., Heinrich, J. G. and Li, D.,2012. Scan pattern, stress and mechanical strength of laser directly sintered ceramics. The International Journal of Advanced Manufacturing Technology, 64(1-4), pp.239-246.

Shishkovsky, I., Yadroitsev, I., Bertrand, P. and Smurov, I., 2007. Alumina–zirconium ceramics synthesis by selective laser sintering/melting. Applied Surface Science, 254(4), pp.966-970.

WU Q, CHEN H, WU J, et al, 2015. Research development of the material used for selective laser sintering. Materials Review, 29(26), pp:78–83.

ONUH S O, YUSUF Y Y, 1999. Rapid prototyping technology:applications and benefits for rapid product development. Journal of Intelligent Manufacturing, 10(3/4), pp:301–311.

JI Hong-chao, ZHANG Xue-jing, PEI Wei-chi, et al, 2018. Research Progress in Ceramic 3D Printing Technology and Material Development. Journal of Materials Engineering, 46(7), pp:19-28.

R. Vaidyanathan, J. Walish, J.L., et al, 2000. The Extrusion Freeforming of Functional Ceramic Prototypes. JOM, 52(12), pp.34-37.

Powell J, Assabumrungrat S, Blackburn S, 2013. Design of ceramic paste formulations for co-extrusion. Powder Technology, 245, pp.21-27.

Imen Grida, Julian R.G. and Evans, 2003. Extrusion freeforming of ceramics through fine nozzles. Journal of the European Ceramic Society, 23(5), pp.629-635.

Ming C L, Jie L and Hilmas G E, 2015. Effects of Temperature on Aqueous Freeform Extrusion Fabrication. Solid Freedom Fabrication Symposium, pp.319-331.

Li W, Ghazanfari, ALeu M, et al, 2015. Methods of extrusion on demand for high solids loading ceramic paste in freeform extrusion fabrication. Solid Freedom Fabrication Symposium, pp.332-345.

Syed Ali Ashter, 2013. Other Processing Approaches. In: Thermoforming of Single and Multilayer Laminates. pp.229–260.

LI Yaogang, YE Xiaomeng, JI Hongchao, et al, 2019. Design and Optimization of the Screw Extrusion Device for a Precursor Ceramic Material 3D Printer. Journal of Beijing University of Technology, 45(12), pp.1173-1180.

Zhang X F, Yu G Q, Jiang L W, 2010. Application of Alumina Ceramic. Foshan Ceramics, 20(2), pp.38-43.

Li Jiang, Pan Yubo, Ning Jinwei et al, 2001. Low temperature sintering of alumina ceramics. China Ceramics, 37(5), pp.42-45.

Yu Pan, He Li, Yongsheng Liu, et al, 2020. Effect of Holding Time During Sintering on Microstructure and Properties of 3D Printed Alumina Ceramics. Frontiers in Materials, pp.1-12.

Akira Nakajima and Gary L. Messing, 1996. Liquid-phase sintering of alumina coated with magesium aluminosilicate glass. J. Am. Geram. Soc, 79(12), pp.199-210.

Liptak, Bela G, 2005. Instrument Engineers' Handbook: Process Control and Optimization. CRC Press. pp. 2464. ISBN 978-0-8493-1081-2.

Shan Zhengqiang et al, 2000. Gearbox Stepped Motor. Electrical World, pp. 1-2.